reflected the losses that subjects acquired before getting a large reward. However, we also ran a regression analysis using losses and found significant correlation in the ventroanterior region of the insula. Anatomical and physiological studies of the insula also showed involvement of its ventroanterior part in perception of aversive stimuli[17]. Thus we argue that the activation of dorsoposterior insula is not simply due to losses in the LONG condition.

Previous brain imaging and neural recording studies suggest a role for the striatum in prediction and processing of reward[9,10,14,21,24–29]. Consistent with previous fMRI studies[8,11,16], our results showed striatal activity correlated with the error of reward prediction. Reinforcement learning models of the basal ganglia[13–15] posit that the striatum learns reward prediction and action selection based on the reward prediction error $\delta(t)$ represented by the dopaminergic input. Correlation of striatal activity with reward prediction error $\delta(t)$ could be due to dopamine-dependent plasticity of cortico-striatal synapses[30].

In lateral OFC, DLPFC, PMd, IPC and dorsal raphe, we found significant activations in the block-design analyses, but we did not find strong correlation in regression analyses. This may be because these areas perform functions that are helpful for reward prediction and action selection, but their activities do not directly represent the amount of predicted reward or prediction error at a specific time scale.

In reinforcement learning theory, an optimal action selection is realized by taking the action a that maximizes the 'action value' $Q(s, a)$ at a given state s. The action value is defined as $Q(s,a) = E[\, r(s,a) + \gamma\, V(s'(s, a))]$ and represents the expected sum of the immediate reward $r(s, a)$ and the weighted future rewards $V(s'(s, a))$, where $s'(s, a)$ means the next state reached by taking an action a at a state s (refs. 12,15). According to this framework, we can see that prediction of immediate reward $r(s, a)$ is helpful for action selection based on rewards at either short or long time scales, that is, with any value of the discount factor γ. On the other hand, prediction of state transition $s'(s, a)$ is helpful only in long-term reward prediction with positive values of γ.

In the lateral OFC, we observed significant activity in both the SHORT versus NO and the LONG versus NO contrasts (**Supplementary Table 1** online), but no significant correlation with reward prediction $V(t)$ or reward prediction error $\delta(t)$ in regression analysis. This suggests that the lateral OFC takes the role of predicting immediate reward $r(s, a)$, which is used for action selection in both SHORT and LONG conditions, but not in the NO condition. This interpretation is consistent with previous studies demonstrating the OFC's role in prediction of rewards, immediately following sensorimotor events[31,32], and action selection based on reward prediction[23,33,34].

In the DLPFC, PMd and IPC, there were significant activations in both the LONG versus NO and the LONG versus SHORT contrasts (**Supplementary Table 1** online) but no significant correlation with either $V(t)$ or $\delta(t)$. A possible interpretation is that this area is involved in prediction of future state $s'(s, a)$ in the LONG condition but not in the SHORT or NO conditions. This interpretation is consistent with previous studies showing the role of these cortical areas in imagery[35], working memory and planning[36,37].

The dorsal raphe nucleus was activated in the LONG versus SHORT contrast, but was not correlated with $V(t)$ or $\delta(t)$. In consideration of its serotonergic projection to the cortex and the striatum and serotonin's implication with behavioral impulsivity[4–6], a possible role for the dorsal raphe nucleus is to control the effective time scale of reward prediction[7]. Its higher activity in the LONG condition, where a large setting of γ is necessary, is consistent with this hypothesis.

Let us consider the present experimental results in light of the anatomy of cortico-basal ganglia loops (illustrated in **Supplementary Fig. 2**). The cortex and the basal ganglia both have parallel loop organization, with four major loops (limbic, cognitive, motor and oculomotor) and finer, topographic sub-loops within each major loop[38]. Our results suggest that the areas within the limbic loop[39], namely the lateral OFC and ventral striatum, are involved in immediate reward prediction. On the other hand, areas within the cognitive and motor loops[38], including the DLPFC, IPC, PMd and dorsal striatum, are involved in future reward prediction. The connections from the insula to the striatum are topographically organized, with the ventral-anterior, agranular cortex projecting to the ventral striatum and the dorsal-posterior, granular cortex projecting to the dorsal striatum[19] (see **Supplementary Fig. 2**). The graded maps shown in **Figure 6b,c** are consistent with this topographic cortico-striatal organization and suggest that areas that project to the more dorsoposterior part of the striatum are involved in reward prediction at a longer time scale. These results are consistent with the observations that localized damages within the limbic and cognitive loops manifest as deficits in evaluation of future rewards[1,3,34,40,41] and learning of multi-step behaviors[42]. The parallel learning mechanisms in the cortico-basal ganglia loops used for reward prediction at a variety of time scales may have the merit of enabling flexible selection of a relevant time scale appropriate for the task and the environment at the time of decision making.

A possible mechanism for selection or weighting of different cortico-basal ganglia loops with an appropriate time scale is serotonergic projection from the dorsal raphe nucleus[7] (see **Supplementary Fig. 2**), which was activated in the LONG versus SHORT contrast. Although serotonergic projection is supposed to be diffuse and global, differential expression of serotonergic receptors in the cortical areas and in the ventral and dorsal striatum[43,44] would result in differential modulation. The mPFC, which had significant correlation with reward prediction $V(t)$ at long time scales ($\gamma \geq 0.6$), may regulate the activity of the raphe nucleus through reciprocal connection[45,46]. This interpretation is consistent with previous studies using tasks that require long-range prospects for problem solving, such as the gambling problem[1] or delayed reward task[2], which showed involvement of the medial OFC. Future studies using the Markov decision task under pharmacological manipulation of the serotonergic system should clarify the role of serotonin in regulating the time scale of reward prediction.

Recent brain imaging and neural recording studies report involvement of a variety of cortical areas and the striatum in reward processing[8–11,16,21,23–29,32,33,47–49]. Although some neural recording studies have used experimental tasks that require multiple trial steps for getting rewards[47,48], none of the previous functional brain imaging studies addressed the issue of reward prediction at different time scales, and considered only rewards immediately following stimuli or actions. We were able extract specific functions of OFC, DLPFC, mPFC, insula and cortico-basal ganglia loops using our new Markov decision task and a reinforcement learning model–based regression analysis. Our regression analysis not only extracted brain activities specific to reward prediction, but also revealed a topographic organization in reward prediction (**Fig. 6**). The combination of our Markov decision task with event-related fMRI and magnetoencephalography (MEG) should further clarify the functions used for reward prediction and perception at different time scales, and at finer spatial and temporal resolutions.

METHODS

Subjects. Twenty healthy, right-handed volunteers (18 males and 2 females, ages 22–34 years) gave informed consent to participate in the experiment, which was conducted with the approval of the ethics and safety committees of Advanced Telecommunication Research Institute International (ATR) and Hiroshima University.

Behavioral task. In the Markov decision task (Fig. 1), one of three states was visually presented to the subject using three different shapes, and the subject selected one of two actions by pressing one of two buttons using their right hand (Fig. 1a). The rule of state transition was the same for all conditions: $s_3 \rightarrow s_2 \rightarrow s_1 \rightarrow s_3 \ldots$ for action a_1, and $s_1 \rightarrow s_2 \rightarrow s_3 \rightarrow s_1 \rightarrow \ldots$ for action a_2. The rules for reward, however, changed in each condition. In the SHORT condition (Fig. 1b), action a_1 results in a small positive reward ($+r_1$ = 10, 20 or 30 yen, with equal probabilities), whereas action a_2 results in a small loss ($-r_1$) at any of the three states. Thus, the optimal behavior is to collect small positive rewards at each state by performing action a_1. In the LONG condition (Fig. 1c), however, the reward setting is such that action a_2 gives a large positive reward ($+r_2$ = 90, 100 or 110 yen) at state s_3, and action a_1 gives a large loss ($-r_2$) at state s_1. Thus, the optimal behavior is to receive small losses at states s_1 and s_2 to obtain a large positive reward at state s_3 by taking action a_2 at each state. There were two control conditions: the NO condition, where the reward was always zero, and the RANDOM condition, where the reward was positive ($+r_1$) or negative ($-r_1$) with equal probability, regardless of state or action.

Subjects completed 4 trials in a NO condition block, 15 trials in a SHORT condition block, 4 trials in a RANDOM condition block and 15 trials in a LONG condition block. A set of four condition blocks (NO, SHORT, RANDOM, LONG) was repeated four times (Fig. 2a). Subjects were informed of the current condition at the beginning of each condition block by text on the screen (first slide in Fig. 1a); thus, the entire experiment consisted of 168 steps (152 trial steps and 16 instruction steps), taking about 17 min. The mappings of the three states to the three figures, and the two buttons to the two actions, were randomly set at the beginning of each experiment, so that subjects were required to learn the amount of reward associated with each figure-button pair in both SHORT and LONG conditions. Furthermore, in the LONG condition, subjects had to learn the subsequent figure for each figure-action pair and take into account the amount of reward expected from the subsequent figure in selecting a button.

fMRI imaging. A 1.5-tesla scanner (Shimadzu-Marconi, Magnex Eclipse) was used to acquire both structural T1-weighted images (repetition time, TR = 12 ms, TE = 4.5 ms, flip angle = 20°, matrix = 256 × 256, FoV = 256 mm, thickness = 1 mm, slice gaP = 0 mm) and T2*-weighted echo planar images (TR = 6 s, TE = 55 ms, flip angle = 90°, 50 transverse slices, matrix = 64 × 64, FoV = 192 mm, thickness = 3 mm, slice gap = 0 mm) showing blood oxygen level–dependent (BOLD) contrasts.

Because the aim of the present study was to identify brain activity underlying reward prediction over multiple trial steps, we acquired functional images every 6 s (TR = 6 s), in synchrony with single trials. Although shorter TRs and event-related designs are often used in experiments that aim to distinguish brain responses to events within a trial[9,11,21,26], analysis of those finer events in time were not the focus of the current study. With this longer TR, the BOLD signal in a single scan contained a mixture of responses for a reward-predictive stimulus and reward feedback. However, because of the progress of learning and the stochastic nature of the amount of reward, the time courses of reward prediction $V(t)$ and prediction error $\delta(t)$ over the 168 trial steps were markedly different. Thus, we could separate activity corresponding to reward prediction from that corresponding to outcomes by using both reward prediction $V(t)$ and reward outcome $r(t)$ in multiple regression analysis, as described below.

Data analysis. The data were pre-processed and analyzed with SPM99 (www.fil.ion.ucl.ac.uk/spm/spm99.html). The first two volumes of images were discarded to avoid T1 equilibrium effects. The images were realigned to the first image as a reference, spatially normalized with respect to the Montreal Neurological Institute EPI template, and spatially smoothed with a Gaussian kernel (8 mm, full-width at half-maximum).

We conducted two types of analysis. One was block-design analysis using four boxcar regressors covering the whole experiment, convolved with a hemodynamic response function as the reference waveform for each condition (NO, SHORT, RANDOM, LONG). We did not find substantial differences between SHORT versus NO and SHORT versus RANDOM contrasts, or between LONG versus NO and LONG versus RANDOM contrasts. Therefore we report here only the results with the NO condition as the control condition. The other method was multivariate regression analysis using explanatory variables, representing the time course of the reward prediction $V(t)$ or reward prediction error $\delta(t)$ at six different timescales γ, estimated from subjects' performance data (described below).

In both analyses, images of parameter estimates for the contrast of interest were created for each subject. These were then entered into a second-level group analysis using a one-sample t test at a threshold of $P < 0.001$, uncorrected for multiple comparisons (random effects analysis) and extent threshold of four voxels. Small-volume correction (SVC) was done at a threshold of $P < 0.05$ using an ROI within the striatum (including the caudate and putamen), which was defined anatomically based on a normalized T1 image.

Procedures of performance-based regression analysis. The time courses of reward prediction $V(t)$ and reward prediction error $\delta(t)$ were estimated from each subject's performance data—state $s(t)$, action $a(t)$ and reward $r(t)$—as described below.

Reward prediction. To estimate how much of a forthcoming reward a subject would have expected at each step during the Markov decision task, we took the definition of the value function (equation 1) and reformulated it based on the recursive structure of the task. Namely, if the subject starts from a state $s(t)$ and comes back to the same state after k steps, the expected cumulative reward $V(t)$ should satisfy the consistency condition $V(t) = r(t + 1) + \gamma\, r(t + 2) + \ldots + \gamma^{k-1} r(t + k) + \gamma^k V(t)$.

Thus, for each time t of the data file, we calculated the weighted sum of the rewards acquired until the subject returned to the same state and estimated the value function for that episode as

$$\hat{V}(t) = \frac{\left[r(t+1) + \gamma r(t+2) + \Lambda + \gamma^{k-1} r(t+k)\right]}{1-\gamma^k} \qquad (1)$$

The estimate of the value function $V(t)$ at time t was given by the average of all previous episodes from the same state as at time t

$$V(t) = \frac{1}{L}\sum_{l=1}^{L} \hat{V}(t_l) \qquad (2)$$

where $\{t_1, \ldots, t_L\}$ are the indices of time visiting the same state as $s(t)$, that is, $s(t_1) = \ldots = s(t_L) = s(t)$.

Reward prediction error. The TD error (equation 2) was calculated from the difference between the actual reward $r(t)$ and the temporal difference of the estimated value function $V(t)$.

We separately calculated the time courses of $V(t)$ and $\delta(t)$ during SHORT and LONG conditions; we concatenated data of four blocks in the SHORT condition, and calculated $V(t)$ and $\delta(t)$ as described above. We used the same process for the LONG condition data. During the NO and RANDOM conditions, the values of $V(t)$ and $\delta(t)$ were fixed at zero. Finally, we reconstructed the data corresponding to the real time course of the experiment. Examples of the time course of these variables are shown in Supplementary Figure 1 online. We used either $V(t)$ or $\delta(t)$ as the explanatory variable in a regression analysis by SPM. To remove any effects of factors other than reward prediction, we concurrently used other variables in the regression, namely the four box-car functions representing each condition (NO, SHORT, RANDOM, LONG). Because the immediate reward prediction $V(t)$ with $\gamma = 0$ can coincide with reward outcome $r(t)$ if learning is perfect, we included the reward outcome $r(t)$ in regression analyses with $V(t)$. Thus, the significant correlation with $V(t)$ (Fig. 6a,b) should represent a predictive component rather than a reward outcome.

The amplitude of explanatory variables $\delta(t)$ with all γ were large in early trials and decreased as subjects learned the task (Supplementary Fig. 1 online). This decreasing trend causes a risk that areas that are activated early in trials, such as those responsible for general attentiveness or novelty, have correlations with $\delta(t)$. Because our aim in regression analysis was to clarify the brain structures involved in reward prediction at specific time scales, we removed the areas that had similar correlation to $\delta(t)$ at all settings of γ from considerations in Figure 6 and Supplementary Table 3 online. To compare the results of regression analysis

with six different values of γ, we used display software that can overlay multiple activation maps in different colors on a single brain structure image. When a voxel is significantly activated in multiple values of γ, it is shown by a mosaic of multiple colors, with apparent subdivision of the voxel (Fig. 6).

Note: Supplementary information is available on the Nature Neuroscience website.

ACKNOWLEDGMENTS

We thank K. Samejima, N. Schweighofer, M. Haruno, H. Imamizu, S. Higuchi, T. Yoshioka, T. Chaminade and M. Kawato for helpful discussions and technical advice. This research was funded by 'Creating the Brain,' Core Research for Evolutional Science and Technology (CREST), Japan Science and Technology Agency.

COMPETING INTERESTS STATEMENT

The authors declare that they have no competing financial interests.

Received 5 March; accepted 2 June 2004
Published online at http://www.nature.com/natureneuroscience/

1. Bechara, A., Damasio, H. & Damasio, A.R. Emotion, decision making and the orbitofrontal cortex. *Cereb. Cortex* **10**, 295–307 (2000).
2. Mobini, S. *et al.* Effects of lesions of the orbitofrontal cortex on sensitivity to delayed and probabilistic reinforcement. *Psychopharmacology (Berl.)* **160**, 290–298 (2002).
3. Cardinal, R.N., Pennicott, D.R., Sugathapala, C.L., Robbins, T.W. & Everitt, B.J. Impulsive choice induced in rats by lesions of the nucleus accumbens core. *Science* **292**, 2499–2501 (2001).
4. Rogers, R.D. *et al.* Dissociable deficits in the decision-making cognition of chronic amphetamine abusers, opiate abusers, patients with focal damage to prefrontal cortex, and tryptophan-depleted normal volunteers: evidence for monoaminergic mechanisms. *Neuropsychopharmacology* **20**, 322–339 (1999).
5. Evenden, J.L. & Ryan, C.N. The pharmacology of impulsive behaviour in rats: the effects of drugs on response choice with varying delays of reinforcement. *Psychopharmacology (Berl.)* **128**, 161–170 (1996).
6. Mobini, S., Chiang, T.J., Ho, M.Y., Bradshaw, C.M. & Szabadi, E. Effects of central 5-hydroxytryptamine depletion on sensitivity to delayed and probabilistic reinforcement. *Psychopharmacology (Berl.)* **152**, 390–397 (2000).
7. Doya, K. Metalearning and neuromodulation. *Neural Net.* **15**, 495–506 (2002).
8. Berns, G.S., McClure, S.M., Pagnoni, G. & Montague, P.R. Predictability modulates human brain response to reward. *J. Neurosci.* **21**, 2793–2798 (2001).
9. Breiter, H.C., Aharon, I., Kahneman, D., Dale, A. & Shizgal, P. Functional imaging of neural responses to expectancy and experience of monetary gains and losses. *Neuron* **30**, 619–639 (2001).
10. O'Doherty, J.P., Deichmann, R., Critchley, H.D. & Dolan, R.J. Neural responses during anticipation of a primary taste reward. *Neuron* **33**, 815–826 (2002).
11. O'Doherty, J.P., Dayan, P., Friston, K., Critchley, H. & Dolan, R.J. Temporal difference models and reward-related learning in the human brain. *Neuron* **38**, 329–337 (2003).
12. Sutton, R.S. & Barto, A.G. *Reinforcement Learning* (MIT Press, Cambridge, Massachusetts, 1998).
13. Houk, J.C., Adams, J.L. & Barto, A.G. in *Models of Information Processing in the Basal Ganglia* (eds. Houk, J.C., Davis, J.L. & Beiser, D.G.) 249–270 (MIT Press, Cambridge, Massachusetts, 1995).
14. Schultz, W., Dayan, P. & Montague, P.R. A neural substrate of prediction and reward. *Science* **275**, 1593–1599 (1997).
15. Doya, K. Complementary roles of basal ganglia and cerebellum in learning and motor control. *Curr. Opin. Neurobiol.* **10**, 732–739 (2000).
16. McClure, S.M., Berns, G.S. & Montague, P.R. Temporal prediction errors in a passive learning task activate human striatum. *Neuron* **38**, 339–346 (2003).
17. Mesulam, M.M. & Mufson, E.J. Insula of the old world monkey. III: Efferent cortical output and comments on function. *J. Comp. Neurol.* **212**, 38–52 (1982).
18. Cavada, C., Company, T., Tejedor, J., Cruz-Rizzolo, R.J. & Reinoso-Suarez, F. The anatomical connections of the macaque monkey orbitofrontal cortex. *Cereb. Cortex* **10**, 220–242 (2000).
19. Chikama, M., McFarland, N.R., Amaral, D.G. & Haber, S.N. Insular cortical projections to functional regions of the striatum correlate with cortical cytoarchitectonic organization in the primate. *J. Neurosci.* **17**, 9686–9705 (1997).
20. Balleine, B.W. & Dickinson, A. The effect of lesions of the insular cortex on instrumental conditioning: evidence for a role in incentive memory. *J. Neurosci.* **20**, 8954–8964 (2000).
21. Knutson, B., Fong, G.W., Bennett, S.M., Adams, C.M. & Hommer, D. A region of mesial prefrontal cortex tracks monetarily rewarding outcomes: characterization with rapid event-related fMRI. *Neuroimage* **18**, 263–272 (2003).
22. Ullsperger, M. & von Cramon, D.Y. Error monitoring using external feedback: specific roles of the habenular complex, the reward system, and the cingulate motor area revealed by functional magnetic resonance imaging. *J. Neurosci.* **23**, 4308–4314 (2003).
23. O'Doherty, J., Critchley, H., Deichmann, R. & Dolan, R.J. Dissociating valence of outcome from behavioral control in human orbital and ventral prefrontal cortices. *J. Neurosci.* **23**, 7931–7939 (2003).
24. Koepp, M.J. *et al.* Evidence for striatal dopamine release during a video game. *Nature* **393**, 266–268 (1998).
25. Elliott, R., Friston, K.J. & Dolan, R.J. Dissociable neural responses in human reward systems. *J. Neurosci.* **20**, 6159–6165 (2000).
26. Knutson, B., Adams, C.M., Fong, G.W. & Hommer, D. Anticipation of increasing monetary reward selectively recruits nucleus accumbens. *J. Neurosci.* **21**, RC159 (2001).
27. Pagnoni, G., Zink, C.F., Montague, P.R. & Berns, G.S. Activity in human ventral striatum locked to errors of reward prediction. *Nat. Neurosci.* **5**, 97–98 (2002).
28. Elliott, R., Newman, J.L., Longe, O.A. & Deakin, J.F. Differential response patterns in the striatum and orbitofrontal cortex to financial reward in humans: a parametric functional magnetic resonance imaging study. *J. Neurosci.* **23**, 303–307 (2003).
29. Haruno, M. *et al.* A neural correlate of reward-based behavioral learning in caudate nucleus: a functional magnetic resonance imaging study of a stochastic decision task. *J. Neurosci.* **24**, 1660–1665 (2004).
30. Reynolds, J.N. & Wickens, J.R. Dopamine-dependent plasticity of corticostriatal synapses. *Neural Net.* **15**, 507–521 (2002).
31. Tremblay, L. & Schultz, W. Reward-related neuronal activity during go-nogo task performance in primate orbitofrontal cortex. *J. Neurophysiol.* **83**, 1864–1876 (2000).
32. Critchley, H.D., Mathias, C.J. & Dolan, R.J. Neural activity in the human brain relating to uncertainty and arousal during anticipation. *Neuron* **29**, 537–545 (2001).
33. Rogers, R.D. *et al.* Choosing between small, likely rewards and large, unlikely rewards activates inferior and orbital prefrontal cortex. *J. Neurosci.* **19**, 9029–9038 (1999).
34. Rolls, E.T. The orbitofrontal cortex and reward. *Cereb. Cortex* **10**, 284–294 (2000).
35. Hanakawa, T. *et al.* The role of rostral Brodmann area 6 in mental-operation tasks: an integrative neuroimaging approach. *Cereb. Cortex* **12**, 1157–1170 (2002).
36. Owen, A.M., Doyon, J., Petrides, M. & Evans, A.C. Planning and spatial working memory: a positron emission tomography study in humans. *Eur. J. Neurosci.* **8**, 353–364 (1996).
37. Baker, S.C. *et al.* Neural systems engaged by planning: a PET study of the Tower of London task. *Neuropsychologia* **34**, 515–526 (1996).
38. Middleton, F.A. & Strick, P.L. Basal ganglia and cerebellar loops: motor and cognitive circuits. *Brain Res. Brain Res. Rev.* **31**, 236–250 (2000).
39. Haber, S.N., Kunishio, K., Mizobuchi, M. & Lynd-Balta, E. The orbital and medial prefrontal circuit through the primate basal ganglia. *J. Neurosci.* **15**, 4851–4867 (1995).
40. Eagle, D.M., Humby, T., Dunnett, S.B. & Robbins, T.W. Effects of regional striatal lesions on motor, motivational, and executive aspects of progressive-ratio performance in rats. *Behav. Neurosci.* **113**, 718–731 (1999).
41. Pears, A., Parkinson, J.A., Hopewell, L., Everitt, B.J. & Roberts, A.C. Lesions of the orbitofrontal but not medial prefrontal cortex disrupt conditioned reinforcement in primates. *J. Neurosci.* **23**, 11189–11201 (2003).
42. Hikosaka, O. *et al.* Parallel neural networks for learning sequential procedures. *Trends Neurosci.* **22**, 464–471 (1999).
43. Mijnster, M.J. *et al.* Regional and cellular distribution of serotonin 5-hydroxytryptamine2a receptor mRNA in the nucleus accumbens, olfactory tubercle, and caudate putamen of the rat. *J. Comp. Neurol.* **389**, 1–11 (1997).
44. Compan, V., Segu, L., Buhot, M.C. & Daszuta, A. Selective increases in serotonin 5-HT1B/1D and 5-HT2A/2C binding sites in adult rat basal ganglia following lesions of serotonergic neurons. *Brain Res.* **793**, 103–111 (1998).
45. Celada, P., Puig, M.V., Casanovas, J.M., Guillazo, G. & Artigas, F. Control of dorsal raphe serotonergic neurons by the medial prefrontal cortex: involvement of serotonin-1A, GABA(A), and glutamate receptors. *J. Neurosci.* **21**, 9917–9929 (2001).
46. Martin-Ruiz, R. *et al.* Control of serotonergic function in medial prefrontal cortex by serotonin-2A receptors through a glutamate-dependent mechanism. *J. Neurosci.* **21**, 9856–9866 (2001).
47. Hikosaka, K. & Watanabe, M. Delay activity of orbital and lateral prefrontal neurons of the monkey varying with different rewards. *Cereb. Cortex* **10**, 263–271 (2000).
48. Shidara, M. & Richmond, B.J. Anterior cingulate: single neuronal signals related to degree of reward expectancy. *Science* **296**, 1709–1711 (2002).
49. Matsumoto, K., Suzuki, W. & Tanaka, K. Neuronal correlates of goal-based motor selection in the prefrontal cortex. *Science* **301**, 229–232 (2003).

Eur Arch Psychiatry Clin Neurosci (2004) 254 : 245–251

DOI 10.1007/s00406-004-0488-z

Shuji Asahi · Yasumasa Okamoto · Go Okada · Shigeto Yamawaki · Norio Yokota

Negative correlation between right prefrontal activity during response inhibition and impulsiveness: A fMRI study

Received: 5 May 2003 / Accepted: 8 December 2003

Abstract Behavioral disinhibition in Go/No-Go task is thought to be associated with impulsiveness in humans. Recent imaging studies showed that neural circuits involving diverse areas of the frontal cortex and other association cortex sites such as the parietal cortex are implicated in the inhibition of response during No-Go trials. The aim of the present study was to investigate the association between regional cerebral activation during No-Go trials and impulsiveness. Seventeen right-handed healthy volunteers participated in the study. We used functional magnetic resonance imaging to measure the brain activation during a Go/No-Go task. The Barratt Impulsiveness Scale, 11th version (BIS-11) was used to measure impulsiveness. Activated regions included the right middle frontal gyrus and the inferior parietal lobe, which is consistent with previous neuroimaging studies. A negative correlation was observed between the motor impulsiveness of BIS-11 and No-Go-related activation in the right dorsolateral prefrontal cortex (RDLPFC). Our results suggest that the RDLPFC is the area most sensitive to differences in individual motor impulsiveness and its activity may be an indicator of the individual capacity for response inhibition.

Key words response inhibition · fMRI · right dorsolateral prefrontal cortex (RDLPFC) · impulsiveness · BIS

Sh. Asahi · Y. Okamoto · G. Okada · Sh. Yamawaki, M.D., Ph.D. (✉)
Department of Psychiatry and Neurosciences
Graduate School of Biomedical Sciences
Hiroshima University
1-2-3 Kasumi, Minami-ku
Hiroshima, 734-8551, Japan
Tel.: +81-82/257-5205
Fax: +81-82/257-5209
E-Mail: yamawaki@hiroshima-u.ac.jp

N. Yokota
Hiroshima Prefectural College of Health and Welfare
Hiroshima, 723-0053, Japan

Introduction

Impulsiveness is a dimensional personality trait that is important for a wide range of different human behaviors. Although a strict definition of impulsiveness is difficult to establish, biological, psychological and social studies have regarded impulsiveness as 'a predisposition toward rapid, unplanned reactions to internal or external stimuli without regard to the negative consequences of these reactions to the impulsive individual or to others' [34]. Recent laboratory investigations of impulsiveness showed two dominant models: (1) *Reward-delay impulsivity*, which is the inability to delay reward and leads to an increased tendency to choose immediate small rewards over larger delayed ones [35]; and (2) *Rapid-response impulsivity*, which is the inability to conform responses to environmental context and leads to errors of commission on tests that require careful checking of stimuli [16]. The latter model appeared to be more closely related to trait impulsiveness, which was measured by the Barratt Impulsiveness Scale (BIS), a popular self-reporting impulsiveness scale [37], and was increased in subjects with a lifetime Axis I or Axis II diagnosis [49].

The ability to inhibit behavioral responses that are inappropriate in the current context is a response inhibition essential for normal behavior, and is thought to be associated with *Rapid-response impulsivity* in humans. This inhibitory function has been investigated frequently using the Go/No-Go task, in which the participants are required to refrain from responding to designated items within a series of stimuli. The prefrontal cortex (PFC) has been implicated in behavioral inhibition, based on animal, clinical and neuroimaging studies. Studies in monkeys demonstrated that lesions in the PFC resulted in difficulties in behavioral inhibition [8, 24, 45], as well as the studies of patients with lesions in the same region [22]. Recent neuroimaging studies using PET or fMRI have shown a right hemispheric dominance of inhibitory control that involves diverse areas of

the frontal cortex and other association cortex sites, such as the parietal cortex, which are implicated in response inhibition during No-Go trials [21, 26, 30]. Although human impulsiveness was revealed to associate with some biological markers [1, 17, 42, 50], the region of the brain that is directly correlated with human impulsiveness is still unclear.

Some experiments used only behavioral laboratory measurements of impulsiveness [11, 21], which do not incorporate the cognitive or social aspects of impulsiveness and do not measure long-term patterns of behavior. This may explain the inconsistency in the findings of those previous studies [9, 33, 38]. Another way to examine impulsiveness is to use self-reporting measurements such as BIS, which has the advantage of generating information on a variety of types of acts and on whether these acts continue as long-term patterns of behavior. In general, a closer association and a greater consistency has been demonstrated among different self-report impulsiveness scales [3, 9, 15].

The aim of the present study was to clarify the brain areas associated with impulsiveness, as measured by BIS-11. Based on the studies cited above, we hypothesized that the degree of activation in some areas within the right hemispheric dominance of neural networks was correlated with the degree of impulsiveness.

Methods

Subjects

Seventeen right-handed healthy volunteers (10 men and 7 women), aged 23–30 years (mean: 25.1 years), and with no history of neurological or psychiatric illness, participated in the study. Handedness was assessed by the Edinburgh Handedness Inventory [36]. The subjects were recruited from the Kansai area in Japan and were paid ¥7,000 for their participation in the study. The study was conducted under a protocol that was approved by the Ethics Committee of Hiroshima University School of Medicine. All subjects submitted informed written consent of their participation.

Barratt Impulsiveness Scale, 11th version

The BIS-11 [37], a short questionnaire designed to measure impulsiveness, has been validated in impulsive and normal populations. The questionnaire contains a total of 30 items, each of which is answered on a 4-point Likert scale (rarely/never = 1, occasionally = 2, often = 3, almost always/always = 4), and the level of impulsiveness is calculated by summing up the scores for each item. All items are defined as identifying impulsiveness within the structure of related personality traits and are divided into three subscales: attention (inattention and cognitive instability), motor (motor impulsiveness and lack of perseverance), and non-planning (lack of self-control and intolerance of cognitive complexity). The Japanese version of the BIS-11 was developed using a back-translation method and was judged to be a reliable and valid measure in the Japanese population [47]. Subjects completed the BIS-11 after the task procedure.

Experimental tasks

The task consisted of eight alternating 36-s epochs of Go and No-Go conditions. During the experiment, subjects viewed a series of letters once every 1500 ms and responded with a key press to every letter except the letter 'X', to which they were instructed to withhold response. All subjects responded using the forefinger of the right hand. Stimulus duration was 500 ms and the interstimulus interval was 1000 ms for both conditions. Subjects were instructed to try to respond while the stimulus was on the screen. In the Go (control) condition, subjects were presented a random sequence of letters other than the letter 'X'. In the No-Go condition, subjects were presented with the letter 'X' 50 % of the time, thus requiring a response to half the trials (Go trials) and a response inhibition to the other half (No-Go trials). The high frequency of targets was maintained across the entire experiment, which generated a compelling tendency to respond. In order to ensure correct performance, the subjects were trained outside the task scanner until they understood the task completely. Motor responses were made using a fiber-optic response pad (Current Designs Inc, Philadelphia). The task consisted of eight blocks, each of which continues without being preceded by an instruction. The subjects could not distinguish the boundary between the conditions; therefore, different strategies are not imposed on the subject for the different conditions.

fMRI acquisition

Functional magnetic resonance imaging (fMRI) was performed using a Magnex Eclipse 1.5T Power Drive 250 (Marconi Medical Systems, USA). A time-course series of 107 volumes was acquired with T2*-weighted, gradient echo, echo planar imaging (EPI) sequences. Each volume consisted of 38 slices, and the slice thickness was 4.0 mm with no gap to cover the entire cerebral and cerebella cortex. The interval between two successive acquisitions of the same image (TR) was 4000 ms, echo time (TE) was 55 ms, and the flip angle was 90°. The field of view was 256 mm, and the matrix size was 64×64, giving voxel dimensions of $4.0 \times 4.0 \times 4.0$ mm. After functional scanning, structural scans were acquired using Tl-weighted gradient echo pulse sequence (TR = 12 ms; TE = 4.5 ms; Flip angle = 20°; FOV = 256 mm; voxel dimensions of $1.0 \times 1.0 \times 1.0$ mm), which facilitated the localization and coregistration of functional data.

Analysis

The image data were analyzed by statistical parametric mapping (SPM99 software from the Wellcome Department of Cognitive Neurology, London, UK) implemented in Matlab (Mathworks Inc., Sherborn, MA). The first three volumes of each fMRI run (prescan period) were discarded because the magnetization was unsteady. The remaining 104 volumes were used for the statistical analysis. Images were corrected for motion and realigned, using the first scan of the session as a reference. T1 anatomical images were coregistered to the first functional scans and aligned to the T1 template included in SPM99. The calculated nonlinear transformation was applied to all functional images for spatial normalization. Finally, the functional images were smoothed with an 8 mm full-width, half-maximum (FWHM) Gaussian filter. Using group analysis according to a random effect model [18], we identified regions that showed significant responses to the No-Go condition compared with that of the Go condition as areas related to response inhibition. The group analysis consisted of two levels. In the first level, the signal time course of each subject was modeled with a delayed box-car function convolved with a hemodynamic response function in the context of a general linear model. One contrast image per subject was created by contrasting the No-Go conditions with the Go conditions. These images were entered into a one-sample t-test, which allowed us to identify regions of the brain that were significantly activated by the response inhibition function during the No-Go condition as compared to the Go condition. The resulting foci were then characterized in terms of spatial extent (k) and peak height (u). The significance of each region was estimated using distribution approximations from the theory of Gaussian fields. This characterization is in terms of the probability that a region of the observed number of voxels (or greater) could have occurred by chance (extent threshold) over the entire volume analyzed. After locating and analyzing areas of the brain that showed sig-

nificant activation during the No-Go condition, we then performed a regression analysis on these areas only, to determine the association between the magnitude of brain activation in each area and the scores of the BIS-11. Activations were reported if they exceeded $p < 0.001$ (uncorrected) on the single voxel level and $p < 0.05$ (corrected) on the cluster level. In regression analysis, we masked with the regions that showed significant responses to the No-Go condition compared with that of the Go condition, as the areas related to response inhibition described above, to avoid identifying regions that were not activated for the No-Go condition compared with the Go condition. However, when using a lower threshold, an activation that was at a lower level but consistent with the significant activation noted above was seen over more widespread areas of the brain. This occurred because the threshold for this mask was set at $p < 0.05$ and larger areas are included in the final analysis of the response inhibition data. Therefore, significance was considered at a threshold of $p < 0.001$ and an extent of > 40 contiguous voxels. Labels for brain activation foci were obtained in Talairach coordinates using the Talairach Demon software, which provides an accuracy similar to that of neuroanatomical experts [28].

Behavioral analysis

Errors of commission (response to 'X') and omission (not to response to targets) were recorded, and the average response times to targets were calculated for each subject.

Results

Behavioral and BIS-11 results

Subjects performed well on the task, making a few commission errors (7.3 %) and a few omission errors (1.3 %). The response times to targets averaged 325.8 ± 20.8 ms. Average scores of the total BIS-11, attention-key, motor-key and non-planning-key were 68.9 ± 11.0, 19.7 ± 3.3, 21.1 ± 4.1 and 28.1 ± 5.3, respectively. Some correlation was detected among the BIS-11 scales. The total score of BIS-11 was strongly correlated with all of the 3 subscales (attention-key: $r = 0.69$, $p < 0.01$; motor-key: $r = 0.89$, $p < 0.01$; non-planning-key: $r = 0.93$, $p < 0.01$). Among the subscales, the non-planning-key and attention-key ($r = 0.51$, $p < 0.05$), or non-planning-key and motor-key ($r = 0.79$, $p < 0.01$) were correlated. There was also a trend between attention-key and motor-key, though not significant ($r = 0.48$, $p = 0.05$). These results were natural because the BIS-11 has sufficient internal consistency reliability [47]. No correlation was observed between the performance data (i. e., number of commission errors or omission errors, average response time to targets) and the BIS-11 scores.

fMRI data

For fMRI data analysis, the threshold for activation was set at $p < 0.001$ for voxel level. In Fig. 1 and Table 1, the activation, which was corrected for multiple comparisons at the extent threshold of $p < 0.05$, is shown. Four independent areas of activation, which were predominantly right-lateralized, were observed to underlie response inhibition. These areas, including the Talairach coordinates of their centers-of-mass, are presented in Table 1. The No-Go condition, in comparison to the Go condition, resulted in the significant activation of the right middle and superior temporal gyrus, the right precentral gyrus, the right middle frontal gyrus, and the right cuneus and precuneus.

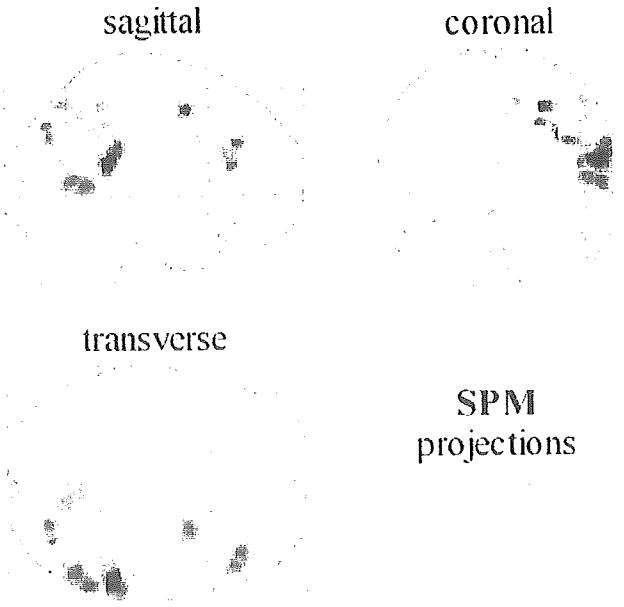

Fig. 1 Statistical parametric maps of brain regions (on the second level group analysis for the 17 subjects) showing significant activation associated with the NO-GO condition, compared with the GO condition at a statistical threshold of $P < 0.001$ (uncorrected) on the single voxel level and $P < 0.05$ (corrected) on the cluster level. For exact coordinates, see Table1. Clusters of activation are shown as through-projections onto representations of standard stereotactic space. *Sagittal* side view; *coronal* view from back; *transverse* view from above

Regression analysis revealed a significant negative correlation between the motor-key score of BIS-11 and the magnitude of brain activation during response inhibition in the right middle frontal gyrus (x, y, z = 34, 22, 29; area 9; t-value = 5.66; 42 voxels; $r = -0.93$; $p < 0.01$) showed in Fig. 2A, B. Other BIS-11 scores (i. e., total BIS-11, attention-key and non-planning-key) did not show a significant association with the magnitude of brain activation during response inhibition. Furthermore, no significant correlation was observed between the performance data (i. e., the number of commission errors and omission errors, response time) and the magnitude of brain activation during response inhibition.

By analyzing the mean percentage signal changes in the regions shown in Fig. 1 and Table 1, we sought to find the possible functional connectivity among the regions concerning response inhibition. Consequently, we detected a correlation between the areas including the right middle frontal/the right precentral gyrus and the right cuneus/precuneus ($r = 0.65$, $p < 0.01$). There was no correlation between the other regions.

Table 1 Brain areas significantly activated during response inhibition

Area	BA	Cluster level		Voxel level		x	y	z
		p	k	p	T			
R superior temporal gyrus	22	0.000	1193	0.003	9.82	58	−42	18
R middle temporal gyrus	37			0.095	7.05	60	−52	8
R middle temporal gyrus	37			0.153	6.67	52	−60	10
R middle frontal gyrus	6	0.003	276	0.133	6.78	26	4	50
R precentral gyrus	9			0.983	4.42	44	12	38
R middle frontal gyrus	9	0.005	258	0.177	6.55	40	34	30
R middle frontal gyrus	46			0.288	6.15	48	30	18
R middle frontal gyrus	46			0.639	5.38	52	26	26
R cuneus	7	0.001	332	0.230	6.34	24	−76	40
R cuneus	19			0.292	6.14	34	−74	34
R precuneus	7			0.596	5.46	10	−66	52

The names of areas described above point to the peaks of activation within each cluster
p corrected p values for spatial extent (cluster level p value) and peak height (voxel level p value) of the activation: all areas exceeding the corrected cluster level threshold of 0.05 are displayed; *k* number of voxels in cluster; *T* t score; *x, y, z* localization according to the standard Talairach coordinates (in mm); *L* left; *R* right

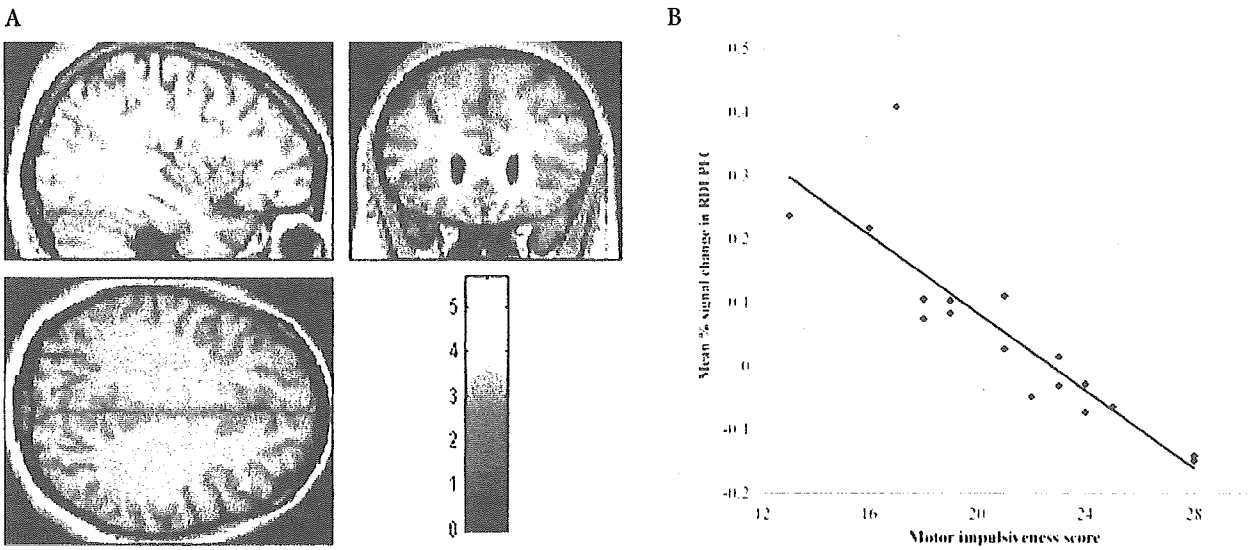

Fig. 2 **A** Statistical parametric maps of brain region (on the regression analysis for the 17 subjects) showing significant activation negatively associated with the motor-key score of BIS-11, within the areas activated during response inhibition, at a statistical threshold of $P < 0.05$ (uncorrected) on the single voxel level and $P < 0.05$ (corrected) on the cluster level. The region corresponds to the RDLPFC: x, y, z = 34, 22, 29; area 9; t-value = 5.66; 42 voxels. Clusters of activation are shown as through-projections onto representations of standard stereotactic space. *Sagittal* side view; *coronal* view from back; *transverse* view from above. **B** Correlation between mean percentage of signal change within the RDLPFC shown in Fig. 2A and the motor-key scores of BIS-11. The correlation coefficient is $r = -0.93$; $p < 0.01$

Discussion

In the present study, we examined the brain areas associated with impulsiveness as measured by BIS-11 in healthy volunteers. We have shown a significant negative correlation between the motor-key score of BIS-11 and the magnitude of activation in the right dorsolateral prefrontal cortex (RDLPFC) during the No-Go condition compared to that of the Go condition (i. e., as the motor-key score of BIS-11 increases, the signal intensity seen in the region including the RDLPFC decreases). These results suggest that the RDLPFC may play a more important role in response inhibition in motor inhibitory control than other brain regions.

We used BIS-11, a self-report measure, in the assessment of impulsiveness. This scale was designed to measure temperament, a long lasting characteristic of the personality of the subject. In addition, we can gather consistent information that is not affected by experimental methods or tasks. Our results illuminated the motor impulsiveness of BIS-11 as only a subscale, which has a significant association with the activation in the RDLPFC during response inhibition. Although the BIS-11 and its subscales have sufficient internal consistency reliability, other subscales did not show any association

between any brain regions activated during response inhibition. That may be because the Go/No-Go task we employed is a task emphasized on the motor response inhibition. Barratt (1994) reported that college students scored higher on average for motor impulsiveness than a mixed adult population and lower for cognitive impulsiveness, whereas a group of psychiatric inpatients scored high mainly on the non-planning impulsiveness [2]. This indicates that motor impulsiveness is more sensitive than other subscales of BIS (i. e. cognitive impulsiveness and non-planning impulsiveness) in young healthy persons and supports our result, which illuminated motor impulsiveness in our comparatively young (25.1 years old on average) healthy subjects.

In this study, brain activation associated with successful response inhibition was observed as a distributed network in the right hemisphere, which was consistent with the results of previous functional brain imaging studies that suggest right hemisphere regions, including the RDLPFC, the inferior parietal cortex and, medially, the anterior cingulate cortex (ACC), are especially important for inhibitory control [6, 7, 13, 20, 21, 27, 43]. In particular, the importance of the RDLPFC was emphasized after regression analysis. The RDLPFC is one of the most consistently activated areas in regard to inhibitory control, and is thought to participate in the active suppression of inappropriate movement and behavior. The right lateral prefrontal regions have been shown to be activated in countering proactive interference [7], set-shifting involving the inhibition of the previous rule in the Wisconsin Card Sorting task [27], response inhibition in the Stop paradigm [39, 43], suppression of imitative behavior [5], and a range of clinical disinhibition syndromes that follow right hemisphere damage [46, 48]. In addition to being involved in the suppression of movement and behavior, the RDLPFC is also associated with the voluntary suppression of a positive emotional reaction, such as sexual arousal [4], and the voluntary suppression of a negative emotion, such as sadness [29]. These facts indicate that the RDLPFC is a key structure involved in the variety of inhibitory control.

We did not observe any significant correlation between the performance data (i. e., the number of commission errors and omission errors, response time) and the magnitude of brain activation during response inhibition. This result is not consistent with the results of Garavan et al. (1999), which suggest that the faster a subject was in responding to the targets, the greater the signal intensity seen in the regions, including the right inferior frontal cluster and the left inferior parietal lobule cluster, during response inhibition [21]. Comparing our performance data with theirs, the percentage of commission errors and omission errors are almost the same. Therefore, it may be difficult to interpret the inconsistency simply as the task level of difficulty. Another possible interpretation is the difference of strategies in executing the task. The response time to targets and the accuracy of responses are conflicting natures in executing the Go/No-Go task. Both of these parameters may be sensitive and variable to the difference in strategies each subject used to emphasize the response time to targets or the accuracy of responses, when they are demanded to manage both. Actually, the mean response time to targets in our subjects (326 ms) was considerably shorter than that of the subjects in the other study (460 ms).

Casey et al. (1997) showed a significant negative correlation between the number of commission errors and the volume of activation in the orbital frontal gyrus [11]. Regrettably, our experimental conditions did not show a significant activation in the orbitofrontal cortex, as did other fMRI studies. This inconsistency may be due to the difference of methods employed. The correlation the other studies observed maybe reflected the developmental difference between adults and children, because those studies mixed adults and children as subjects in their experiment. In fact, those studies also showed that the volume of activation was significantly greater in children relative to adults when performing the No-Go condition of the task. However, the location of activation in the PFC was not different between the age groups. This observation may be due to susceptibility effects at the air-tissue interface in the perinasal sinuses, which renders orbitofrontal activation difficult to observe in fMRI. However, lesion studies in animals and in humans have traditionally implicated the orbitofrontal cortex in behavioral inhibition [19]. Therefore, we cannot exclude a potential role of the orbitofrontal cortex in inhibitory control based on fMRI data.

Liddle et al. (2001) [30] reported that the activation of ACC during No-Go trials was not substantially greater than that during Go trials under circumstances in which No-Go trials and Go trials were equally probable. In addition, they reported that the activation of ACC was related to decision formation and monitoring, rather than to response inhibition. These results may explain why our results have not shown activation in the ACC. We used a standard blocked design [11] in this study as a way to provide and maintain a high level of prepotent response. Randomly presenting an equal number of Go and No-Go stimuli would have eliminated a buildup of a prepotent response. In such a situation, the subjects were required to make and monitor decisions attentively during both conditions, which might result in little difference between the activation of the ACC during No-Go conditions and that during Go conditions.

In addition to those areas discussed above, we detected activities in other areas including the right middle frontal/the right precentral gyrus (frontal cortex) and the right cuneus/precuneus (parietal cortex). Moreover, a correlation was detected between both areas by analyzing the mean percentage signal changes in the regions during response inhibition. The observed activation in these two areas might be related to motor imagery, which is defined as the mental simulation of a motor act [12, 14], and is reported from neuroimaging studies to share neural substrates with those underlying motor execution [31, 40, 41]. The precentral sulcus at the level of middle

frontal gyrus and the posterior superior parietal/precuneus were reported to be activated more during motor imagery than the motor execution [23] and are thought to correspond to a 'negative motor area' where electrical stimulation causes a cessation of movement [32] because activity for inhibiting movement would be needed during motor imagery. Therefore, our observation that these areas are activated may be reasonable.

One of the most important issues of the present results is why high impulsive subjects perform as well as low impulsive subjects with less activity in the RDLPFC. It may be possible to explain this by the fact that a parametric manipulation of the ratio between Go and No-Go stimuli revealed the RDLPFC increases as inhibitory difficulty decreased, that is, as the relative numbers of No-Go stimuli increased, thereby diminishing response prepotency [10, 13]. That is thought to reflect the importance of maintaining relevant stimulus information against interference from competing non-target stimuli. Therefore, the high impulsive subjects with less activation in the RDLPFC may have less capacity left for response inhibition than that of less impulsive subjects. However, some fMRI studies concerning working memory showed an increased activity in the PFC with increasing memory loads, possibly due to a limited capacity of the system for controlled processing [25, 44]. Therefore, the relationship between the task difficulty and the activation in the PFC may depend on the tasks which require different processes of cognitive functions. Further studies are needed to clarify this issue.

One of the limitations of this study is that a block design was used for investigating motor response suppression. When employing block design, it is difficult to control for the difference in frequency of motor responses between blocks that differ in the proportion of Go and No-Go events. Casey et al. (1997) tried to avoid this difficulty by comparing the epochs containing Go and No-Go responses with two baseline conditions that contained only Go trials. One baseline was established from a frequency of Go trials that matched that in the No-Go condition (ensuring approximate matching of number of motor responses), while the other baseline was established with the total number of trials matching the No-Go condition (ensuring matching of the number of stimuli presented) [11]. Their results showed that the same areas were activated during No-Go conditions and Go conditions in both contrasts. Together, these results may support the validity of our study using the latter baseline. Another possible limitation is in measuring impulsiveness using questionnaires, which are subjective. Shortcomings on self-report measures include the need to rely on the honesty of the individuals completing the questionnaire.

Conclusion

We observed a negative correlation between the motor impulsiveness assessed by BIS-11 and the activation of the RDLPFC during response inhibition in healthy subjects. Our findings highlight the importance of the activity in the RDLPFC as the area most sensitive to the differences in individual motor impulsiveness, even in the healthy subjects. However, the role of the RDLPFC remains unclear, thus, further studies are needed.

References

1. af Klinteberg B, Schalling D, Edman G, Oreland L, Asberg M (1987) Personality correlates of platelet monoamine oxidase (MAO) activity in female and male subjects. Neuropsychobiology 18:89–96
2. Barratt ES (1994) Impulsiveness and aggression. In: Monahan J, Steadman HJ (eds) Violence and mental disorder: developments in risk assessment, Chicago. University of Chicago Press, pp 61–79
3. Barratt ES (1985) Impulsiveness subtraits, arousal and information processing. In: Spence JT, Itard CE (eds) Motivation, emotion and personality. North Holland: Elsevier Science, pp 137–146
4. Beauregard M, Levesque J, Bourgouin P (2001) Neural correlates of conscious self-regulation of emotion. J Neurosci 21:RC165
5. Brass M, Zysset S, von Cramon DY (2001) The inhibition of imitative response tendencies. Neuroimage 14:1416–1423
6. Braver TS, Barch DM, Gray JR, Molfese DL, Snyder A (2001) Anterior cingulate cortex and response conflict: effects of frequency, inhibition and errors. Cereb Cortex 11:825–836
7. Bunge SA, Ochsner KN, Desmond JE, Glover GH, Gabrieli JD (2001) Prefrontal regions involved in keeping information in and out of mind. Brain 124:2074–2086
8. Butters N, Butter C, Rosen J, Stein D (1973) Behavioral effects of sequential and one-stage ablations of orbital prefrontal cortex in the monkey. Exp Neurol 39:204–214
9. Carrillo-de-la-Pena MT, Otero JM, Romero E (1993) Comparison among various methods of assessment of impulsiveness. Percept Mot Skills 77:567–575
10. Casey BJ, Forman SD, Franzen P, Berkowitz A, Braver TS, Nystrom LE, Thomas KM, Noll DC (2001) Sensitivity of prefrontal cortex to changes in target probability: a functional MRI study. Hum Brain Mapp 13:26–33
11. Casey BJ, Trainor RJ, Orendi JL, Schubert AB, Nystrom LE, Giedd JN, Castellanos FX, Haxby JV, Noll DC, Cohen JD, Forman SD, Dahl RE, Rapoport JL (1997) A developmental functional MRI study of prefrontal activation during performance of a go/no-go task. J Cogn Neurol 9:835–847
12. Crammond DJ (1997) Motor imagery: never in your wildest dream. Trends Neurosci 20:54–57
13. de Zubicaray GI, Andrew C, Zelaya FO, Williams SC, Dumanoir C (2000) Motor response suppression and the prepotent tendency to respond: a parametric fMRI study. Neuropsychologia 38: 1280–1291
14. Decety J (1996) The neurophysiological basis of motor imagery. Behav Brain Res 77:45–52
15. Dickman SJ (1990) Functional and dysfunctional impulsivity: personality and cognitive correlates. J Pers Soc Psychol 58: 95–102
16. Evenden JL (1998) The pharmacology of impulsive behaviour in rats IV: the effects of selective serotonergic agents on a paced fixed consecutive number schedule. Psychopharmacology (Berl) 140:319–330
17. Fallgatter AJ, Herrmann MJ (2001) Electrophysiological assessment of impulsive behavior in healthy subjects. Neuropsychologia 39:328–333
18. Friston KJ, Holmes AP, Worsley KJ, (1999) How many subjects constitute a study? Neuroimage 10:1–5
19. Fuster JM (1989) The prefrontal cortex: Anatomy, Physiology and Neuropsychology of the Frontal Lobe. Raven Press, New York, p 110

20. Garavan H, Ross TJ, Murphy K, Roche RA, Stein EA (2002) Dissociable executive functions in the dynamic control of behavior: inhibition, error detection, and correction. Neuroimage 17: 1820–1829
21. Garavan H, Ross TJ, Stein EA (1999) Right hemispheric dominance of inhibitory control: an event-related functional MRI study. Proc Natl Acad Sci USA 96:8301–8306
22. Godefroy O, Rousseaux M (1996) Divided and focused attention in patients with lesion of the prefrontal cortex. Brain Cogn 30: 155–174
23. Hanakawa T, Immisch I, Toma K, Dimyan MA, Van Gelderen P, Hallett M (2003) Functional properties of brain areas associated with motor execution and imagery. J Neurophysiol 89:989–1002
24. Iversen SD, Mishkin M (1970) Perseverative interference in monkeys following selective loss of the inferior prefrontal convexity. Exp Brain Res 11:376–386
25. Jaeggi SM, Seewer R, Nirkko AC, Eckstein D, Schroth G, Groner R, Gutbrod K (2003) Does excessive memory load attenuate activation in the prefrontal cortex? Load-dependent processing in single and dual tasks: functional magnetic resonance imaging study. Neuroimage 19:210–225
26. Kawashima R, Satoh K, Itoh H, Ono S, Furumoto S, Gotoh R, Koyama M, Yoshioka S, Takahashi T, Takahashi K, Yanagisawa T, Fukuda H (1996) Functional anatomy of GO/NO-GO discrimination and response selection – A PET study in man. Brain Research 728:79–89
27. Konishi S, Nakajima K, Uchida I, Kikyo H, Kameyama M, Miyashita Y (1999) Common inhibitory mechanism in human inferior prefrontal cortex revealed by event-related functional MRI. Brain 122:981–991
28. Lancaster JL, Woldorff MG, Parsons LM, Liotti M, Freitas CS, Rainey L, Kochunov PV, Nickerson D, Mikiten SA, Fox PT (2000) Automated Talairach atlas labels for functional brain mapping. Hum Brain Mapp 10:120–131
29. Levesque J, Eugene F, Joanette Y, Paquette V, Mensour B, Beaudoin G, Leroux JM, Bourgouin P, Beauregard M (2003) Neural circuitry underlying voluntary suppression of sadness. Biol Psychiatry 53:502–510
30. Liddle PF, Kiehl KA, Smith AM (2001) Event-related fMRI study of response inhibition. Hum Brain Mapp 12:100–109
31. Lotze M, Montoya P, Erb M, Hulsmann E, Flor H, Klose U, Birbaumer N, Grodd W (1999) Activation of cortical and cerebellar motor areas during executed and imagined hand movements: an fMRI study. J Cogn Neurosci 11:491–501
32. Luders HO, Dinner DS, Morris HH, Wyllie E, Comair YG (1995) Cortical electrical stimulation in humans. The negative motor areas. Adv Neurol 67:115–129
33. Milich R, Kramer J (1984) Reflections on impulsivity: an empirical investigation of impulsivity as a construct. Advances in Learning and Behavioral Disabilities 3:57–94
34. Moeller FG, Barratt ES, Dougherty DM, Schmitz JM, Swann AC (2001) Psychiatric aspects of impulsivity. Am J Psychiatry 158: 1783–1793
35. Monterosso J, Ainslie G (1999) Beyond discounting: possible experimental models of impulse control. Psychopharmacology (Berl) 146:339–347
36. Oldfield RC (1971) The assessment and analysis of handedness: the Edinburgh inventory. Neuropsychologia 9:97–113
37. Patton JH, Stanford MS, Barratt ES (1995) Factor structure of the Barratt impulsiveness scale. J Clin Psychol 51:768–774
38. Paulsen K, Johnson M (1980) Impulsivity: a multidimensional concept with developmental aspects. J Abnorm Child Psychol 8: 269–277
39. Pliszka SR, Liotti M, Woldorff MG (2000) Inhibitory control in children with attention-deficit/hyperactivity disorder: event-related potentials identify the processing component and timing of an impaired right-frontal response-inhibition mechanism. Biol Psychiatry 48:238–246
40. Porro CA, Cettolo V, Francescato MP, Baraldi P (2000) Ipsilateral involvement of primary motor cortex during motor imagery. Eur J Neurosci 12:3059–3063
41. Porro CA, Francescato MP, Cettolo V, Diamond ME, Baraldi P, Zuiani C, Bazzocchi M, di Prampero PE (1996) Primary motor and sensory cortex activation during motor performance and motor imagery: a functional magnetic resonance imaging study. J Neurosci 16:7688–7698
42. Reist C, Helmeste D, Albers L, Chhay H, Tang SW (1996) Serotonin indices and impulsivity in normal volunteers. Psychiatry Res 60:177–184
43. Rubia K, Russell T, Overmeyer S, Brammer MJ, Bullmore ET, Sharma T, Simmons A, Williams SC, Giampietro V, Andrew CM, Taylor E (2001) Mapping motor inhibition: conjunctive brain activations across different versions of go/no-go and stop tasks. Neuroimage 13:250–261
44. Rypma B, Berger JS, D'Esposito M (2002) The influence of working-memory demand and subject performance on prefrontal cortical activity. J Cogn Neurosci 14:721–731
45. Sasaki K, Gemba H, Tsujimoto T (1989) Suppression of visually initiated hand movement by stimulation of the prefrontal cortex in the monkey. Brain Res 495:100–107
46. Shulman KI (1997) Disinhibition syndromes, secondary mania and bipolar disorder in old age. J Affect Disord 46:175–182
47. Someya T, Sakado K, Seki T, Kojima M, Reist C, Tang SW, Takahashi S (2001) The Japanese version of the Barratt Impulsiveness Scale, 11th version (BIS-11): its reliability and validity. Psychiatry Clin Neurosci 55:111–114
48. Starkstein SE, Robinson RG (1997) Mechanism of disinhibition after brain lesions. J Nerv Ment Dis 185:108–114
49. Swann AC, Bjork JM, Moeller FG, Dougherty DM (2002) Two models of impulsivity: relationship to personality traits and psychopathology. Biol Psychiatry 51:988–994
50. Walderhaug E, Lunde H, Nordvik JE, Landro NI, Refsum H, Magnusson A (2002) Lowering of serotonin by rapid tryptophan depletion increases impulsiveness in normal individuals. Psychopharmacology (Berl) 164:385–391

Eur Arch Psychiatry Clin Neurosci

DOI 10.1007/s00406-004-0538-6

ORIGINAL PAPER

Hidehisa Yamashita · Yasumasa Okamoto · Shigeru Morinobu · Shigeto Yamawaki · Seppo Kähkönen

Visual emotional stimuli modulation of auditory sensory gating studied by magnetic P50 suppression

Received: 18 November 2003 / Accepted: 11 June 2004 / Published online: 12 November 2004

Abstract The auditory sensory gating system modulates its sensitivity to incoming stimuli and prevents higher brain functions from sensory overload in the primary auditory cortex. We investigated whether visually evoked emotional stimuli affect auditory sensory gating. Magnetic P50 (P50m) suppression was evaluated by magnetoencephalography in fifteen healthy subjects while they viewed slides varying in emotional valence and arousal. The ratio of strength of dipole moments of the 2nd to the 1st P50m and the anatomical location of their sources were calculated. Negatively valenced slides significantly attenuated P50m suppression, as compared to neutral ones, while the effects of positive slides were insignificant. No effects on latencies or the location of P50m sources were observed. Thus, negative emotional stimuli may modulate sensory gating.

Key words emotion · auditory sensory gating · magnetoencephalography (MEG) · P50 suppression

H. Yamashita (✉)
1-2-3, Kasumi, Minami-ku
Hiroshima 734–8551, Japan
Tel.: +81-82/257-5208
Fax: +81-82/257-5209
E-Mail: hidehisa@hiroshima-u.ac.jp

H. Yamashita · Y. Okamoto · S. Morinobu · S. Yamawaki
Department of Psychiatry and Neurosciences
Graduate School of Biomedical Sciences
Hiroshima University, Japan

H. Yamashita · Y. Okamoto · S. Morinobu · S. Yamawaki
Core Research for Evolutional Science and Technology (CREST) of Japan Science and Technology Corporation (JST)

S. Kähkönen
BioMag Laboratory
Medical Engineering Center
Helsinki University Central Hospital, Finland

S. Kähkönen
Cognitive Brain Research Unit
Department of Psychology
University of Helsinki, Finland

Introduction

Sensory gating is defined as the pre-attentive ability of the brain to modulate its sensitivity to an incoming stimulus, and is hypothesized to be a protective mechanism that prevents sensory overload of higher brain functions by filtering out the irrelevant sensory input (Braff and Geyer 1990). Deficit in sensory gating could result in an overload of irrelevant stimuli, which in turn may lead to perceptual and attentional impairments associated with psychiatric disorders such as schizophrenia (McGhie and Chapman 1961).

A paired click paradigm is used to evaluate the auditory sensory gating. In this paradigm, two identical stimuli (1st: conditioning stimulus and 2nd: test stimulus) are presented with a short inter-stimulus interval (ISI) of 500 ms and a longer inter-pair interval. The P50 appears as a positive peak in electroencephalography (EEG), at about 50 ms after the stimulus onset. Under normal conditions the amplitude of the P50 for test stimuli is smaller than that for conditioning stimuli, and this suppression of P50 is typically quantified as a ratio (S2/S1). This phenomenon is referred to as P50 suppression (Adler et al. 1982).

Magnetoencephalography (MEG) offers a non-invasive method for functional brain studies with high temporal resolution equal to that of EEG, but it enables more accurate source localization. MEG measures selectively the activity from tangential sources and is well suited for the measurement and localization of primary auditory cortical activity (Hämäläinen et al. 1993). MEG studies indicate that the magnetic P50 (P50m) counterpart is generated in the superior aspects of temporal lobes, near the primary auditory cortex (Hari et al. 1980; Reite et al. 1988; Mäkelä et al. 1994).

Cognitive and affective processing are two basic interacting modes of information processing (LeDoux 1993). Several studies have shown that emotional visual stimuli can have an effect on visual evoked potentials (VEPs), especially late component P300 in healthy sub-

EAPCN 538

jects (Lang et al. 1990; Laurian et al. 1991; Kayser et al. 1997; Cuthbert et al. 2000). Only a few studies have investigated the effect of visual emotional stimuli on auditory information processing and have shown that emotional stimuli may in fact affect auditory processing (Schupp et al. 1997; Surakka et al. 1998). However, the exact role of the interaction between emotion and cognition remains to be elucidated. In this study, we examined whether visually evoked emotional stimuli could affect auditory sensory gating, as measured by P50m suppression in healthy subjects.

Methods

Subjects

Fifteen healthy, right-handed volunteers (14 males and 1 female), aged 22–38 years (mean age 29.5 ± 5.1y), participated in the experiment consisting of three sessions in a randomized order. The subjects reported having no history of neurological or psychiatric disorders or of any drug use for 2 weeks before the study. Because acute nicotine ingestion within 0.5 h of testing may alter P50 suppression, subjects were not permitted to smoke at least 1 h before until the end of the measurement (Adler et al. 1992). Informed consent was obtained from each subject according to institutional guidelines, and the study was approved by an institutional ethical committee.

Task procedure

During the MEG recording, the subject sat in a comfortable chair in a magnetically shielded room. The auditory evoked magnetic fields were recorded with a 204 channel MEG (Neuromag Ltd., Finland). The paired-click paradigm with an inter-click interval of 500 ms with click pairs (0.1 ms, 60dB above the individually determined subjective hearing threshold) separated by 8 s inter-pair was used. The stimuli were delivered binaurally to subjects through a non-magnetic, echo-free plastic tube system, because all previous studies which investigated P50 suppression have used bilateral stimuli (Adler et al. 1982; Braff et al. 1990; Adler et al. 1992; Light et al. 1999; Patrick et al. 1999; Adler et al. 2001), and the ipsilateral P50 response to monoaural stimuli is so small that it is difficult to detect. Three hundred digitized pictures (one hundred per category) were chosen from the International Affective Picture System (IAPS) (Lang et al. 1997). The categories were negative, neutral, and positive (e. g., mutilations, buildings, and pleasant landscapes, respectively). The visual stimuli were presented by projection onto a screen during the interval of click pair presentation for 6 s, from 1 s after the second click to 1 s before the first click of the next pair (Fig. 1). The viewing distance was 3 m, and light was dimmed during the measurement. Three sessions were recorded for 15 minutes per session in a randomized order. The subjects rated their experiences evoked by stimuli, on two dimensions: valence and arousal (Lang et al. 1997). The ratings were made on a nine-point visual analog scale. The valence scale varied from unhappy to happy. The arousal scale varied from calm to highly arousing.

Neuroimaging data collection

The position of the subject's head relative to the recording instrument was determined by measuring the magnetic fields produced by marker coils in relation to cardinal points of the head (nasion, left and right pre-auricular points), which were determined before the experiment using an Isotrack 3D-digitizer (Polhemus, Colchester, VT, U. S. A.) (Ahlfors and Ilmoniemi 1989). The recording passband was 0.1–200 Hz for MEG and EOG, and the sampling rate was 600.025 Hz. Digital band-pass filtering was performed off-line at 5–50 Hz (Light et al. 1999). The first few responses and the entire epoch coinciding with EOG or MEG changes exceeding 150 μV or 3000 ft/cm, respec-

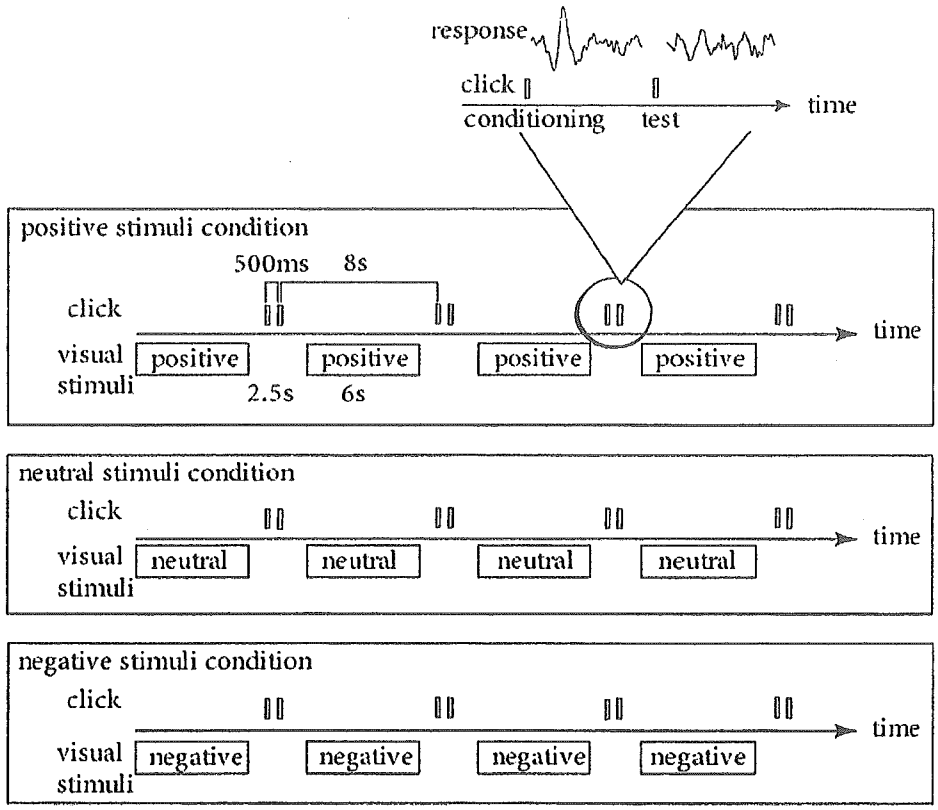

Fig. 1 Schematic diagram of the stimulus sequences in the three experimental conditions. Auditory stimuli (60dBHL, click: depicted as bars) were presented as trains of pairs in a conditioning (1st)-testing (2nd) paradigm. The inter-pair interval was 500 ms and the intra-pair interval was 8 s. The rectangles below the sounds represent visual stimuli. The visual stimuli were presented during the interval of click pairs presentation for 6 s, from 1 s after the second click to 1 s before the first click of the next pairs. Three sessions (negative, neutral, and positive slide conditions) were recorded separately

tively, were omitted from averaging. An epoch lasted 550 ms, including a 100 ms prestimulus baseline. Electrodes were attached below the right eye and above the left eye to minimize potential electrooculogram artifacts. The electrode impedances were below 5 kΩ. Subjects were monitored visually for signs of sleep. At least, 70 responses were averaged in each condition.

MEG source localization

All analyses were conducted blind to the session condition. An individual sphere model of the head was constructed from the local radius of curvature on the basis of individual MRI images. MRI was performed using a 1.5-T apparatus (General Electric Co., Milwaukee, WI, USA). The P50m peaks were obtained from the latency ranges of 35–80 ms after the stimulus presentation. The latency, location, and strength of the P50m source were analyzed with single equivalent current dipole modeling, determined by a least-squares fit using a subset of 34 channels separately over each auditory cortex (Hämäläinen et al. 1993). Dipole fits with at most 40 % residual variance and with at most 4186 mm^3 confidence volume (10 mm radius sphere) were considered successful. The latency, location and dipole moments of P50m for conditioning stimuli (Qc) and test stimuli (Qt), and the t/c ratio (Qt/Qc) in the positive and negative slide conditions were compared to those in the neutral slide condition.

Data analysis

For statistical analysis, one or two-way analyses of variance (ANOVA) for repeated measures were used. Fisher's PLSD was used for post-hoc tests. Stepwise forward multiple regression analysis was used to examine the Qc, Qt, and t/c ratio-related factors. Qc, Qt, and t/c ratio were entered into the analysis as a dependent variable. Sex, age, hemisphere, valence, and arousal during individual sessions (negative, neutral, and positive) in all subjects were entered as independent variables. In addition, the relationships between the three dependent variables and independent variables were investigated. The results are expressed as a mean ± standard deviation.

Results

The self-ratings of experiences evoked by the positive, neutral, and negative slide sessions were, respectively, 7.3 ± 0.6, 4.8 ± 0.5, and 2.2 ± 0.6 for valence; and 4.4 ± 1.1, 4.2 ± 1.0, and 7.5 ± 0.9 for arousal. A one-way ANOVA revealed a significant main effect of slide category on valence ratings ($F[2,28] = 286.4$; $p < 0.01$). Post-hoc tests showed that all the pair-wise differences were significant ($p < 0.01$). For arousal ratings ANOVA also showed a significant main effect of slide category ($F[2,28] = 67.8$; $p < 0.01$). Post-hoc test showed that the negative slides were experienced as significantly more arousing, in comparison to neutral or positive slides ($p < 0.01$).

Fig. 2 shows the typical response waveform over the left primary auditory cortex and dipole location in one

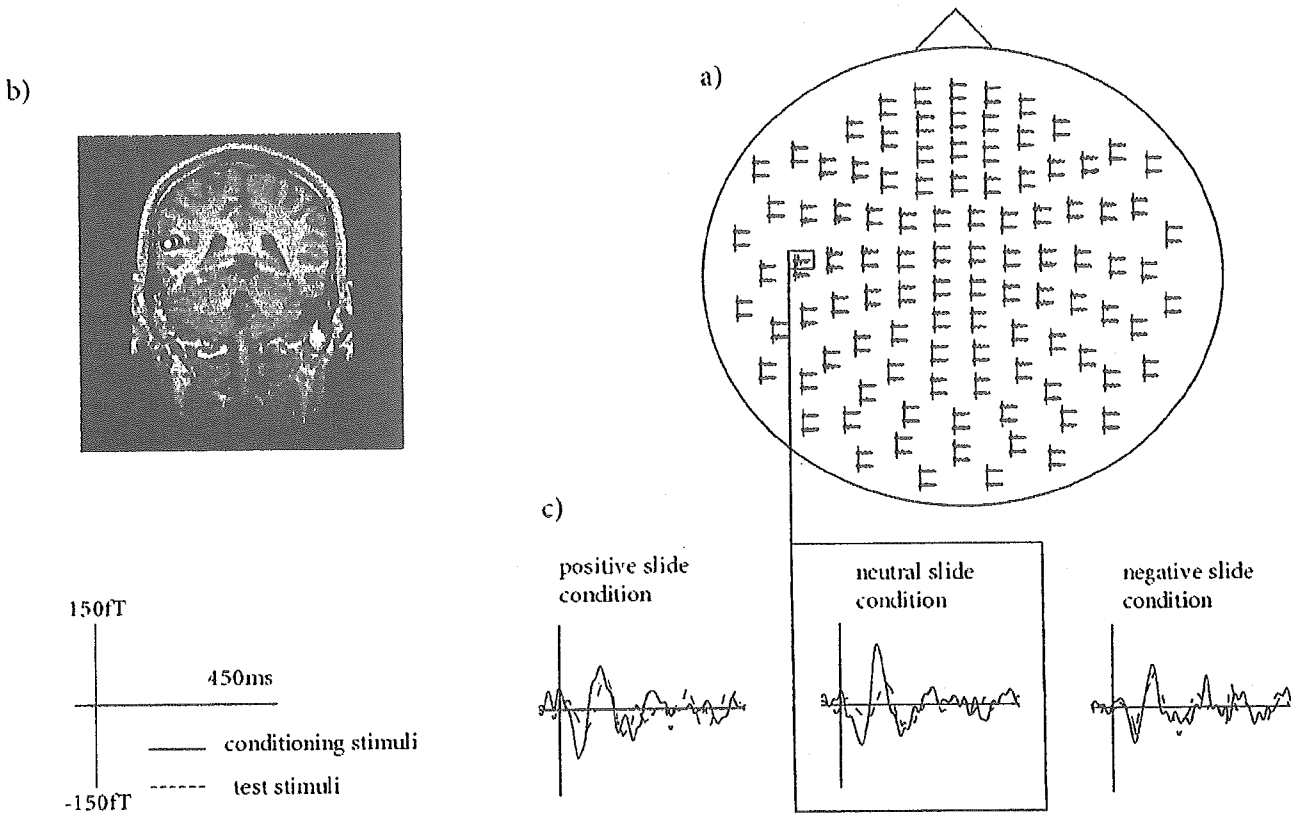

Fig. 2 **a** The average response waveform in the neutral slide condition of one representative subject. **b** Dipole locations over the left primary auditory cortex of one representative subject. The white dot represents the dipole to the conditioning click and the gray dot represents the dipole to the test click. **c** The response waveform at the channel showing maximal response in the left hemisphere in negative (left), neutral (middle), and positive slide conditions (right). The solid line represents the response to the conditioning click and the dashed line, the response to the test click. Note that the amplitude of response waveforms do not directly reflect the intensity of the underlying neural activation, which was estimated on the basis of magnetic field distribution at the sensors and the relative position of the head with respect to the sensors

subject. A significant difference between Qc and Qt in the neutral slide condition was observed in both hemispheres (left: $t=7.85$; $p<0.01$, right: $t=5.19$; $p<0.01$). The strength of Qc was not affected significantly by the slide category or hemisphere. A two-way ANOVA revealed a significant main effect of the slide category on Qt ($F[2,48]=4.27$; $p<0.05$), and t/c ratio ($F[2,48]=15.97$; $p<0.01$), and a significant main effect of hemisphere on t/c ratio ($F[1,24]=6.29$; $p<0.05$). Post-hoc tests showed that Qt and t/c ratio in the negative slide condition were larger than those in the positive and the neutral slide conditions, and t/c ratio in the right hemisphere was larger than that in the left hemisphere (Table 1). Slide category x hemisphere interactions were not significant in any of the analyses. P50m latencies and the source location were not significantly influenced by emotional condition (data not shown).

Table 2 shows the predictors of Qc, Qt, and the t/c ratio. There was no significant predictor of the dipole moment of the Qc response. A stepwise forward multiple regression analysis revealed that the self-rating valence of the emotional slides may have been predictive of dipole moment of Qt response, and t/c ratio and right hemisphere predicted a higher t/c ratio. The relationship between the separate independent variables and the dependent variables is shown in Table 3. The self-rating valence of the emotional slides was significantly correlated with the Qt response, and the t/c ratio. In addition, the t/c ratio was positively correlated with arousal by the emotional slides.

Table 1 Source activations in different emotional conditions

	Slide category		
	Negative	Neutral	Positive
Left hemisphere			
Qc (nAm)	15.0±3.7	18.3±7.4	18.4±6.7
Qt (nAm)	8.9±3.6*	6.0±3.4	6.5±4.2
t/c ratio	0.61±0.24**	0.33±0.17	0.33±0.17
Right hemisphere			
Qc (nAm)	14.0±7.3	16.7±7.6	16.7±7.0
Qt (nAm)	10.7±7.9*	8.0±3.6	7.2±3.9
t/c ratio	0.77±0.25**,[a]	0.48±0.21[a]	0.45±0.22[a]

* $p<0.05$; ** $p<0.01$, compared to Neutral and Positive slide conditions
[a] $p<0.05$, compared to left hemisphere
Qc strength of the P50m response (dipole moment) to conditioning stimuli; *Qt* strength of the P50m response (dipole moment) to test stimuli

Table 2 Multiple regression analysis of predictors of Qc, Qt, and t/c ratio

Independent variables	Coefficient	Standardized coefficient	F	p
Qt				
Valence of stimuli	−0.508	−0.221	4.108	0.046
t/c ratio				
Valence of stimuli	−0.056	−0.454	15.338	< 0.0001
Right hemisphere	0.142	0.268		

There was no significant predictor of dipole moment of Qc response
Qt Multiple $R=0.221$, Multiple $R^2=0.049$, Adjusted $R^2=0.037$
t/c ratio Multiple $R=0.529$, Multiple $R^2=0.280$, Adjusted $R^2=0.261$

Discussion

The present study demonstrated that P50m suppression was attenuated by negative visual stimuli, and that this modulation effect predominated in the right, rather than the left hemisphere, and was related to emotional valence. Our study suggests that negative emotions could modulate sensory gating in the auditory cortex.

A deficit in sensory gating has been identified in a number of psychiatric disorders, most notably schizophrenia (Adler et al. 1982). Furthermore, drugs affecting emotional tone such as amphetamines (Light et al. 1999), marihuana (Patrick et al. 1999), and cocaine (Adler et al. 2001) have been reported to disrupt the P50 suppression. Although emotional stress contributes to the onset and exacerbation of illness in patients with psychiatric disorders, no study has been conducted which attempted to determine the effect of emotional stress on P50 suppression.

There have been a few studies which evaluate the effect of emotional stimuli on other components of event-related potentials (ERP). Schupp et al. (1997) reported that auditory P300 amplitudes were modulated by picture arousal, with smaller auditory P300 responses elicited when viewing highly arousing pictures regardless of their valence. They speculated that attentional resources are needed for the late information processing because they are very complicated and have more cognitive factors. On the other hand, Surakka et al. demonstrated that the mismatch negativity, an ERP component elicited by sound change that peaks about 150 ms after stimulus presentation, was attenuated by positively valenced and little arousing visual emotional stimuli (1998). Our results showed that emotional modulation of sensory processing could occur even at earlier (about

Table 3 Correlations between P50 responses and independent variables

	Qc		Qt		t/c ratio	
	r-value	p-value	r-value	p-value	r-value	p-value
age	−0.054	0.63	−0.063	0.57	−0.055	0.62
sex	0.084	0.45	0.028	0.81	−0.072	0.52
Arousal of stimuli	0.006	0.95	0.205	0.07	0.301	0.006
Valence of stimuli	0.189	0.09	−0.221	0.04	−0.456	< 0.0001

p-values were obtained with Pearson's correlation analysis

50 ms) cortical stages of auditory processing and that this modulation was related to emotional valence. Together, these results suggest that auditory processing can be affected by emotional stimuli, and in earlier stages, the emotional valence of the stimuli may predominate over the arousal effect. However, due to the small sample size, the results should be confirmed by further studies with a larger number of subjects.

The amygdala is thought to play an important role in the perception of emotionally meaningful information (Morris et al. 1996), and neurons in the amygdala of rats behave similarly to the human P50 in response to repeated auditory stimuli (Bordi and LeDoux 1992). In addition, it has been reported that fear conditioning enhances auditory evoked activity in the amygdala in response to repetitive auditory stimuli (Rogan et al. 1997). The amygdala is richly interconnected with the neocortex. Some amygdalofugal projections to auditory areas have been found, in addition to projections to visual regions (Amaral et al. 1992). Thus, we speculate that the effect of emotional visual stimuli on auditory P50m suppression, at least in part, might be mediated by the amygdala.

This P50m suppression study showed that auditory sensory gating at the primary auditory cortex was affected by emotional stimuli, and that this effect may be related more to the emotional valence than to the arousing effect of the stimuli. We suggest that a pre-attentive, automatic mechanism of the brain to gate out incoming irrelevant sensory input is affected by emotional valence.

Acknowledgment This study was supported in part by a Health Science Research Grant for Research on Brain Science from the Ministry of Health, Welfare, and Labor of Japan.

References

1. Adler LE, Hoffer LJ, Griffith J, Waldo MC, Freedman R (1992) Normalization by nicotine of deficient auditory sensory gating in the relatives of schizophrenics. Biol Psychiatry 32:607–616
2. Adler LE, Olincy A, Cawthra E, Hoffer M, Nagamoto HT, Amass L, Freedman R (2001) Reversal of diminished inhibitory sensory gating in cocaine addicts by a nicotinic cholinergic mechanism. Neuropsychopharmacology 24:671–679
3. Adler LE, Pachtman E, Franks RD, Pecevich M, Waldo MC, Freedman R (1982) Neurophysiological evidence for a defect in neuronal mechanisms involved in sensory gating in schizophrenia. Biol Psychiatry 17:639–654
4. Ahlfors S, Ilmoniemi RJ (1989) Magnetometer position indicator for multichannel MEG. In: Williamson SJ, Hoke M, Romani GL (eds) Advance in Biomagnetism, Plenum Press, New York, pp 673–676
5. Amaral DG, Price JL, Pitkänen A, Carmichael ST (1992) Anatomical organization of the primate amygdaloid complex. In: Aggleton JP (eds) The Amygdala: Neurological Aspects of Emotion, Memory, and Mental Dysfunction, Wiley-Liss, New York, pp 1–66
6. Bordi F, LeDoux J (1992) Sensory tuning beyond the sensory system: an initial analysis of auditory response properties of neurons in the lateral amygdaloid nucleus and overlying areas of the striatum. J Neurosci 12:2493–2503
7. Braff DL, Geyer MA (1990) Sensorimotor gating and schizophrenia. Human and animal model studies. Arch Gen Psychiatry 47:181–188
8. Cuthbert BN, Schupp HT, Bradley MM, Birbaumer N, Lang PJ (2000) Brain potentials in affective picture processing: covariation with autonomic arousal and affective report. Biol Psychol 52:95–111
9. Hämäläinen M, Hari R, Ilmoniemi RJ, Knuutila J, Lounasmaa OV (1993) Magnetoencephalography – theory, instrumentation, application to noninvasive studies of working brain. Rev Mod Phys 65:413–498
10. Hari R, Aittoniemi K, Jarvinen ML, Katila T, Varpula T (1980) Auditory evoked transient and sustained magnetic fields of the human brain. Localization of neural generators. Exp Brain Res 40: 237–240
11. Kayser J, Tenke C, Nordby H, Hammerborg D, Hugdahl K, Erdmann G (1997) Event-related potential (ERP) asymmetries to emotional stimuli in a visual half-field paradigm. Psychophysiology 34:414–426
12. Lang PJ, Bradley MM, Cuthbert BN (1997) International Affective Picture System (IAPS). NIMH Center for the Study of Emotion and Attention
13. Lang SF, Nelson CA, Collins PF (1990) Event-related potentials to emotional and neutral stimuli. J Clin Exp Neuropsychol 12: 946–958
14. Laurian S, Bader M, Lanares J, Oros L (1991) Topography of event-related potentials elicited by visual emotional stimuli. Int J Psychophysiol 10:231–238
15. LeDoux JE (1993) Emotional memory systems in the brain. Behav Brain Res 58:69–79
16. Light GA, Malaspina D, Geyer MA, Luber BM, Coleman EA, Sackeim HA, Braff DL (1999) Amphetamine disrupts P50 suppression in normal subjects. Biol Psychiatry 46:990–996
17. Mäkelä JP, Hämäläinen M, Hari R, McEvoy L (1994) Whole-head mapping of middle-latency auditory evoked magnetic fields. Electroencephalogr Clin Neurophysiol 92:414–421
18. McGhie A, Chapman J (1961) Disorders of attention and perception in early schizophrenia. Br J Med Psychol 34:103–116
19. Morris JS, Frith CD, Perrett DI, Rowland D, Young AW, Calder AJ, Dolan RJ (1996) A differential neural response in the human amygdala to fearful and happy facial expressions. Nature 383: 812–815
20. Patrick G, Straumanis JJ, Struve FA, Fitz-Gerald MJ, Leavitt J, Manno JE (1999) Reduced P50 auditory gating response in psychiatrically normal chronic marihuana users: a pilot study. Biol Psychiatry 45:1307–1312
21. Reite M, Teale P, Zimmerman J, Davis K, Whalen J (1988) Source location of a 50 msec latency auditory evoked field component. Electroencephalogr Clin Neurophysiol 70:490–498
22. Rogan MT, Staubli UV, LeDoux JE (1997) Fear conditioning induces associative long-term potentiation in the amygdala. Nature 390:604–607
23. Schupp HT, Cuthbert BN, Bradley MM, Birbaumer N, Lang PJ (1997) Probe P3 and blinks: two measures of affective startle modulation. Psychophysiology 34:1–6
24. Surakka V, Tenhunen-Eskelinen M, Hietanen JK, Sams M (1998) Modulation of human auditory information processing by emotional visual stimuli. Brain Res Cogn Brain Res 7:159–163

Reduced Activation of Posterior Cingulate Cortex During Imagery in Subjects with High Degrees of Alexithymia: A Functional Magnetic Resonance Imaging Study

Tomoyuki Mantani, Yasumasa Okamoto, Naoko Shirao, Go Okada, and Shigeto Yamawaki

Background: *Although the brain areas involved in imagery have been reported, the neural bases of individual differences in imagery remain to be elucidated. People with high degrees of alexithymia (HDA) are known to have constricted imaginal capacities. The purpose of this study was to investigate neural correlates of imagery disturbance in subjects with HDA.*

Methods: *A functional magnetic resonance imaging (fMRI) study was undertaken in 10 subjects with HDA and 10 subjects with low degrees of alexithymia (LDA), who were selected according to their scores on the 20-item Toronto Alexithymia Scale (TAS-20). The two groups' regional cerebral activation was compared during various imagery conditions. In those conditions, the subjects imaged a past happy (PH) event, a past sad (PS) event, a past neutral (PN) event, a future happy (FH) event, a future sad (FS) event, and a future neutral (FN) event. The activation levels during these conditions were compared with those during a rest condition (REST).*

Results: *The t tests showed that the mean subjective ratings of both the vividness of the imagery and the intensity of emotion during the imagery were higher in the subjects with LDA than in those with HDA for the PS and FS imagery conditions. On the other hand, relative to the LDA group, the HDA group showed significantly less activation in the posterior cingulate cortex (PCC) during the PH and FH imagery conditions compared with REST and during the FH imagery condition compared with the FN imagery condition.*

Conclusion: *The present results suggest an association between an HDA and reduced activation of the PCC during happy imagery. Given the function of this brain region, these results might be related to a dysfunction of episodic memory retrieval during happy imagery in subjects with HDA.*

Key Words: Alexithymia, imagery, posterior cingulate cortex, fMRI, future, happy

The brain areas involved in imagery have been investigated by neuroimaging studies in normal subjects. These studies revealed that, in addition to primary and secondary sensory areas (Cabeza and Nyberg 2000; Chen et al 1998; Halpern 2001; Le Bihan et al 1993; Shergill et al 2001; Yoo et al 2003), brain areas with other major cognitive functions, such as language, memory, and movement, are activated during imagery (Mellet et al 1998). The neural bases of individual differences in imagery, however, remain to be elucidated.

Alexithymia, a personality construct, was introduced by Nemiah and Sifneos in the early 1970s. The concept evolved initially from clinical observations of patients with psychosomatic disorders (Nemiah et al 1976). The salient features of this construct are as follows: 1) difficulty identifying and describing subjective feelings; 2) difficulty distinguishing between feelings and bodily sensations of emotional arousal; 3) constricted imaginal capacities; and 4) an externally oriented cognitive style (Nemiah et al 1976). Recently, high prevalences of alexithymia have been reported in various psychiatric disorders, such as somatoform disorders (53%, Cox et al 1994), anxiety disorders (46.7%, Parker et al 1993; 41%, Shipko et al 1983), and substance dependence (51%, Taylor et al 1990). An approximately 10% prevalence has been reported even in normal populations (Honkalampi et al 2000; Salminen et al 1999). Taylor (2000) stated in his review that alexithymia is a deficit in emotional regulation that reflects three kinds of deficits: 1) deficits in the cognitive–experiential component of emotion response systems; 2) deficits at the level of interpersonal regulation of emotion; and 3) constricted imaginal capacities. Several studies have investigated imaginal capacity in people with alexithymia. Nemiah et al (1977) reported that whereas control subjects increased their oxygen consumption when instructed to think various emotional thoughts, subjects with alexithymia showed no such increase in these conditions. Whereas imaginal capacity correlates with hypnotic susceptibility (Varga 2001), Frankel et al (1977) reported a high prevalence of alexithymia in subjects with low hypnotic susceptibility. Hyer et al (1990) studied the responses of posttraumatic stress disorder patients who were listening to accounts of their own traumatic experiences and found that the more alexithymic the subject was, the less his heart rate differed between the stressor period and the baseline. Friedlander et al (1997) compared the responses of people with alexithymia with those of people without it to an autogenic relaxation exercise with guided imagery; the former reported less enjoyment and poorer (less vivid) imagery during relaxation than did the latter. These studies suggest that people with high degrees of alexithymia (HDA) might have low imaginal capacities and show less physical reactivity during imagery with emotional contents; however, these studies relied on indirect methods to characterize the brain function of people with alexithymia.

Imagery can be defined as the manipulation of sensory information that comes from memory without information from actual sensory input (Cabeza and Nyberg 2000). The memory is

From the Department of Psychiatry and Neurosciences, Division of Frontier Medical Science, Programs for Biomedical Research, Graduate School of Biomedical Sciences, Hiroshima University, Hiroshima; and the Core Research for Evolutional Science and Technology (CREST), Japan Science and Technology Corporation (JST), Seika, Japan.

Address reprint requests to Shigeto Yamawaki, M.D., Ph.D., Hiroshima University School of Medicine, Department of Psychiatry and Neurosciences, Division of Frontier Medical Science, Programs for Biomedical Research, Graduate School of Biomedical Sciences, 1-2-3 Kasumi, Minami-ku Hiroshima 734-8551, Japan; E-mail: yamawaki@hiroshima-u.ac.jp.

Received August 11, 2004; revised January 24, 2005; accepted January 28, 2005.

0006-3223/05/$30.00
doi:10.1016/j.biopsych.2005.01.047

BIOL PSYCHIATRY 2005;57:982–990

subdivided into working memory, episodic memory, and semantic memory. Of these subcategories, the one most closely tied to the emotions of daily life is episodic memory, especially "autobiographical memory" (Rubin 1998). Because alexithymia is conceptualized as a multifaceted construct consisting of factors related logically to each other (Taylor et al 1997), the imagery disturbance of alexithymia is considered to be related to other factors, such as difficulty in identifying and describing feelings (i.e., in processing emotion). In fact, experimental studies suggest that imagery disturbance in subjects with alexithymia is related to emotion processing, as mentioned in the previous paragraph. Thus, we considered that subjects with HDA might have difficulty in retrieval of autobiographical memory. On the other hand, the restricted imaginal capacities of people with alexithymia have been considered to limit the extent to which individuals with HDA can modulate anxiety and other emotions by fantasy, dreams, interest, and play (Krystal 1988; Mightes and Cohen 1992). Thus, previous clinical reports have emphasized disturbances in imaging experiences that had not and were not going to occur, as well as past experiences. Furthermore, in examining the types of emotion that accompany imaging, the previous reports seem to have emphasized the difficulty that people with alexithymia have in imaging positive things to modulate negative emotions such as anxiety. So, we planned a functional magnetic resonance imaging (fMRI) study to directly investigate neural correlates of imagery disturbance in the subjects with HDA with the imagery task in which subjects recall affect-laden autobiographical memories or imagine affect-laden future episodes accompanied by positive (happy) or negative (sad) emotions.

Recent positron emission tomography (PET) and fMRI studies have suggested that episodic memory retrieval is associated with activation of the prefrontal, medial–temporal, medial parieto–occipital (posterior cingulate cortex [PCC], including the retrosplenial cortex and precuneus), lateral parietal, anterior cingulate, occipital, and cerebellar regions (Cabeza and Nyberg 2000). On the other hand, it has been reported that the retrieval of autobiographical memory, which is a kind of episodic memory, often activates the medial–frontal region and the left hippocampus and sometimes activates the medial parieto–occipital area (MPOA) (Maguire 2001). These studies suggested a relatively consistent activation of the prefrontal and medial–temporal cortices in episodic/autobiographical memory retrieval; however, there are also inconsistencies among studies of autobiographical memory retrieval, especially regarding the activation of the MPOA. Although several studies have reported the activation of this area (e.g., Maguire and Mummery 1999; Ryan et al 2001), a considerable number have reported no activation of this area (e.g., Conway et al 1999; Markowitsh et al 1997) during the retrieval of autobiographical memory. Meanwhile, emotional stimuli have been reported to consistently activate this area (Maddock 1999). Furthermore, whereas mental imagery is known to be a major component of episodic memory recall (Tulving 1983), MPOA in imagery domain studies seems to be specifically recruited whenever the generation of the mental image relies on the reactivation of a memorized percept (Ghaem et al 1997; Kosslyn et al 1993; Mellet et al 1995; Roland and Gulyas 1995). So, both episodic memory recall and imagery might share the MPOA as a common region. We considered that the inconsistencies concerning the activation of MPOA across studies might reflect not only differences among tasks but also individual differences in personality traits, in individual patterns of reactions to emotional stimuli, or in individual imaginal capacities such as alexithymia. We therefore studied brain activity during imagery in volunteers and investigated the relationship between this brain activity and the level of alexithymia, while paying attention to MPOA (PCC and precuneus; Brodmann's areas 7, 23, 29, 30, 31). We hypothesized that the activation of the MPOA varies with the 20-item Toronto Alexithymia Scale (TAS-20) score during imagery, especially during emotional imagery conditions.

Meanwhile, although no study to date has used neuroimaging techniques to investigate the relationship between brain activation during imagery and alexithymic characteristics, two neuroimaging studies of alexithymia have recently been conducted (Berthoz et al 2002; Kano et al 2003). These studies suggested that there was no difference in the limbic structure between subjects with alexithymia and those without, and that the impairment of anterior cingulate cortex (ACC) functioning might be associated with alexithymia. Moreover, the medial prefrontal cortex (MPFC), adjacent to the ACC, also was activated in numerous neuroimaging studies of emotion (Phan et al 2002) and was reported to be impaired in subjects with alexithymia (Berthoz et al 2002). So, we were also interested in whether the ACC (Brodmann's areas 24, 32, 33) and MPFC (the medial regions of Brodmann's areas 8, 9, 10, 11) are associated with imagery disturbance in subjects with alexithymia.

Methods and Materials

Subjects

We recruited 14 men and six women aged 20–30 years, who were right-handed, nonanxious, and nondepressed (on the basis of Hospital Anxiety and Depression Scale scores; Zigmond and Snaith 1983; Zigmond et al 1993) from among 38 male and 22 female volunteers according to their alexithymia scores on the Japanese version of the TAS-20. The volunteers were recruited through community announcements and were paid incentives corresponding to their transportation expenses. The TAS-20 is the most psychometrically valid and commonly used measurement of alexithymia (Bagby 1994a, 1994b), and the Japanese version also has high construct validity and reliability (Fukunishi et al 1997). It is a self-report questionnaire containing 20 items rated on a 5-point scale. A high score indicates HDA. In accordance with methods used by Berthoz et al (2002), 10 subjects (7 men and 3 women) with high (≥56) TAS-20 scores were placed into an HDA group, and 10 subjects (7 men and 3 women) with lower (≤ 44) scores, who were age- and handedness-matched to the HDA group, were placed into an LDA group. The subjects in the HDA and LDA groups were aged 25.9 ± 3.3 years and 23.7 ± 3.0 years, respectively (mean ± SD), and their TAS-20 scores were 61.9 ± 4.0 and 37.9 ± 3.9, respectively.

All subjects were identified as right-handed according to the Edinburgh inventory (Oldfield 1971). According to the self-reported responses, the subjects had no history of psychiatric, neurologic, or other major medical illness and had never been treated with a psychotropic medication. After the study was described completely to the subjects, written informed consent was obtained from all of them. This study was approved by the Institutional Review Board and the Ethics Committee of Hiroshima University Hospital, Japan. The subjects received course credit for their participation.

Experimental Design

We developed our task by modifying that used in the study by George et al (1995). Before the scanning session, each subject was asked to name specific events that, when imaged, would make him or her happy (one past and one future event) or sad

(one past and one future event). Each subject was also asked to image a specific time when he or she was or would be emotionally neutral—that is, not experiencing any particular emotion (one past and one future event). As for the future events, the subjects were asked to imagine, in the greatest possible detail, specific events that they could realistically expect to occur. The researcher then reviewed each event to assess whether the emotion was appropriate (e.g., not a mixture of happiness and sadness or anger) to the type of event. Additional specific sensory stimuli were elicited that could possibly aid in imaging the event (e.g., the exact place where the subject was or would be at the peak moment of emotion or the clothing, time of year, sights, sounds, or smells associated with that moment). Finally, each subject was asked to supply key words that would simply represent each event (e.g., travel with friends, death of grandmother, brushing teeth).

We used a periodic design involving the presentation of an activation condition for 30 sec followed by a baseline condition for 18 sec. This cycle was repeated 18 times over the course of 864 sec. During the activation condition, subjects were cued by the visual presentation of Japanese words representing the six event conditions: "past happy" (PH), "past sad" (PS), "past neutral" (PN), "future happy" (FH), "future sad" (FS), and "future neutral" (FN); key words were also used to cue the subjects to generate imagery of each event. When the words were presented, the subjects were instructed to image each previously agreed-upon event to make themselves feel the emotions and senses that they would feel as if the past or future event was actually happening. Each word was presented for 30 sec. During the baseline condition (REST), the subjects were shown a cross symbol ("+") and instructed to see only that symbol, with no imagery internally. Each presentation of the symbol lasted 18 sec. During each trial, the words were projected to the center of the subject's field of view with a super video graphics array computer-controlled projection system. The order in which the activation conditions were presented was counterbalanced across the subjects. Each trial was started by presenting the cross symbol for 9 sec; this initial presentation was excluded from the analyses. For each event, each subject's ratings of the vividness of his or her imagery and the intensity of the emotion were recorded immediately after the scanning session. Two nongraduated visual analogue scales were used: one assessed the vividness of the imagery (range, 0–10), from imaging nothing to imaging extremely vividly; and the other assessed the intensity of emotion during the imagery (range, 0–10), from feeling nothing to feeling extremely intensely.

Image Acquisition

Functional magnetic resonance imaging was performed with a Magnex Eclipse 1.5-T Power Drive 250 (Shimadzu Medical Systems, Kyoto, Japan). A time-course series of 291 volumes was acquired with T2-weighted, gradient echo, echo planar imaging sequences. Each volume consisted of 28 slices, with a slice thickness of 4 mm with no gap, and entirely covered the cerebral and cerebellar cortices. The interval between successive acquisitions of the same image (TR) was 3000 msec, the echo time (TE) was 55 msec, and the flip angle was 90°. The field of view (FOV) was 256 mm, and the matrix size was 64 × 64, giving voxel dimensions of 4 × 4 × 4 mm. Scan acquisition was synchronized to the onset of the trial. After functional scanning, structural scans were acquired with a T1-weighted gradient echo pulse sequence (TR = 12 msec; TE = 4.5 msec; flip angle = 20°; FOV = 256 mm; voxel dimensions of 1 × 1 × 1 mm), which facilitated localization.

Analysis

Image processing and statistical analyses were carried out with Statistical Parametric Mapping (SPM99) software (Wellcome Department of Cognitive Neurology, London, United Kingdom) implemented in Matlab (Mathworks, Natick, Massachusetts). The first three volumes of the fMRI run were discarded because the magnetic resonance signal was unsteady. The remaining 288 volumes were used for the analysis. Images were corrected for motion and realigned with the first scan of the session, which served as the reference. For each subject, the T1 anatomic images were coregistered to the first functional images and aligned to a standard stereotaxic space, with the Montreal Neurological Institute (MNI) T1 template in SPM99. The calculated nonlinear transformation was applied to all functional images for spatial normalization. Finally, the functional magnetic resonance images were smoothed with a 10-mm full-width at half-maximum Gaussian filter.

The group analysis was performed at two levels. At the first level, each subject's signal time course was modeled with a delayed boxcar function convolved with a hemodynamic response function in the context of a general linear model. One contrast image per subject was created by contrasting each activation condition (PH, PS, PN, FH, FS, FN) with the baseline condition (REST) and by contrasting each emotional condition with the neutral condition. In the second step, with group analysis according to a random effect model that allows inference to the general source populations (Friston et al 1999), we first identified regions that showed significant responses during each activation condition (PH, PS, PN, FH, FS, FN) compared with the baseline condition (REST) and during each emotional condition compared with the neutral condition (PH > PN, PS > PN, FH > FN, FS > FN) in the HDA and LDA groups, with the one-sample t test. Next, the images were entered into a two-sample t test (to locate brain regions in which the two groups differed significantly) and into a regression analysis (to locate brain regions in which the magnitude of brain activation correlated significantly with the TAS-20 score). Although there were inequalities in the amount of data between the REST condition and the experimental conditions (6 vs. 10), SPM99 performed these analyses, correcting the inequalities of data size. The resulting set of voxel values for each contrast constituted an SPM (t) map. The SPM(t) maps were then interpreted by referring to the probabilistic behavior of Gaussian random fields. The data were thresholded at $p < .001$ uncorrected at the voxel level and at $p < .05$ corrected at the cluster level for regions about which there was no clear hypothesis. Moreover, for regions about which we had an a priori hypothesis (ACC, MPFC, and MPOA), the height and extent of thresholds were set to $p < .001$ uncorrected and $p < .05$ uncorrected, respectively (as justified by Friston 1997).

The x, y, and z coordinates provided by SPM, which were in the MNI brain space, were converted to the x, y, and z coordinates in Talairach and Tournoux's (TT) brain space (Talairach and Tournoux 1988) with the following formula: (TT-x = MNI-x × .88 − .8; TT-y = MNI-y × .97 − 3.32; TT-z = MNI-y × .05 + MNI-z × .88 − .44). Labels for brain activation foci were obtained in Talairach coordinates with Talairach Daemon software (Research Imaging Center, University of Texas, San Antonio, Texas), the accuracy of which is similar to that of neuroanatomic experts (Lancaster et al 2000).

The accuracy of the labeling of the areas given by this software was then confirmed by comparison with activation maps overlaid on MNI-normalized structural magnetic resonance images.

Results

Subjective Ratings

The t tests showed that the mean subjective ratings of the vividness of the imagery were higher in the LDA group than in the HDA group for the PH, PS, and FS conditions. On the other hand, the mean subjective ratings of the intensity of emotion during the imagery were higher in the LDA group than in the HDA group for the PS and FS conditions (Table 1). The examples of the events that subjects imaged during the imagery conditions were sea bathing, party with friends, travel abroad; death of grandmother, death of dog, loss of bag; brushing teeth, cleaning, going to school; honeymoon, playing with child, entrance to ideal occupation; death of mother, loneliness at work, failing to pass on to the next grade; and washing face, changing clothes, driving for PH, PS, PN, FH, FS, FN conditions, respectively. There were no significant differences between the groups in the mean subjective remoteness of the time when the imaged event occurred or would occur in any of the imagery conditions.

fMRI Results (Brain Activation During Imagery Conditions Within Groups)

In the LDA group, at the higher level of significance (height and extent thresholds, respectively, set to $p < .001$ and $p < .05$ corrected), there was significantly greater activation of the PCC in PH and FH than in REST and of the left superior frontal gyrus in PS compared with REST. Moreover, at the lower level of significance (height and extent thresholds, respectively, set to $p < .001$ and $p < .05$ uncorrected), the ACC and right precuneus were significantly more active in PN than in REST and in FH than in FN, respectively. In the HDA group, at the higher level of significance (height and extent thresholds, respectively, set to $p < .001$ and $p < .05$ corrected), there was significantly greater activation of the fusiform gyrus and cerebellum in PH, PN, and FH than in REST (Table 2).

fMRI Results (Comparison of Brain Activation Between Groups)

With the threshold of significance at $p < .001$ uncorrected at the voxel level and at $p < .05$ corrected at the cluster level, FH (FH compared with REST) induced less activation in the HDA subjects than in the LDA subjects in the bilateral PCC (Table 3, Figure 1). These were the only regions showing between-group differences at this level of significance.

Moreover, at the lower level of significance (height and extent thresholds, respectively, set to $p < .001$ and $p < .05$ uncorrected), PH compared with REST and FH compared with FN induced less PCC activation in the HDA group than in the LDA group (Table 3, Figures 2 and 3).

fMRI Results (Regression Analysis)

Regression analysis revealed a significant inverse correlation between the TAS-20 score and the magnitude of brain activation of the bilateral PCC in PH compared with REST (x, y, z = −6, −54, 9; area 30; t value 5.26; 1595 voxels; $r = -.846$; $p < .001$), in FH compared with REST (x, y, z = −8, −50, 9; area 30; t value 7.83; 1363 voxels; $r = -.810$; $p < .001$), and in FH compared with FN (x, y, z = 6, −62, 21; area 31; t value 6.52; 669 voxels; $r = -.812$; $p < .001$) at the higher level of significance (height and extent thresholds, respectively, set to $p < .001$ and $p < .05$ corrected). The Talairach coordinates presented in each parenthesis represents the coordinates in which the local maximum within the cluster was observed. No significant correlation was observed in any other investigated contrasts.

Discussion

As expected, the activation of the MPOA varied with the TAS-20 score (the degrees of alexithymia) during imagery. During FH imagery, the activation in the PCC was significantly lower in the HDA subjects than in the LDA subjects. Also in FH imagery, a significant inverse correlation was found between the TAS-20 score and the magnitude of PCC activation. These results support our hypothesis that the inconsistencies about the activation of MPOA across studies reflect individual differences in personality traits such as alexithymia. The variability of activation in this area according to alexithymic characteristics might explain why prior studies, which did not control for personality, reported various outcomes.

A qualitative comparison of the brain activation detected by one-sample t test in the two groups suggests other findings in addition to the intergroup difference in PCC activation. The LDA

Table 1. Subjective Ratings of Vividness of Imagery and Intensity of Emotion During Imagery

Imagery Condition	TAS-20 Group	Vividness of Imagery			Intensity of Emotion During Imagery		
		Mean	SD	p	Mean	SD	p
Past Happy	HDA	6.1	2.2	.007	6.0	1.8	.068
	LDA	8.3	.75		7.5	1.7	
Past Sad	HDA	4.6	2.7	.031	4.1	2.7	.009
	LDA	7.4	2.6		7.6	2.6	
Past Neutral	HDA	4.2	2.2	.052	2.3	1.9	.188
	LDA	6.3	2.3		3.8	2.8	
Future Happy	HDA	6.5	2.7	.133	5.9	2.7	.086
	LDA	8.1	1.9		7.8	1.8	
Future Sad	HDA	3.9	3.1	.003	3.7	2.8	.010
	LDA	7.7	1.8		7.0	2.4	
Future Neutral	HDA	4.5	2.2	.325	2.3	1.6	.321
	LDA	5.7	2.8		3.5	3.1	

Two nongraduated visual analogue scales were used (the vividness of imagery [imaging nothing to imaging extremely vividly] and the intensity of emotion during imagery [from feeling nothing to feeling extremely intense]). HDA, high degrees of alexithymia group: the subjects with a total 20-item Toronto Alexithymia Scale (TAS-20) score of ≥56; LDA, low degrees of alexithymia group: the subjects with a total TAS-20 score of ≤44; p = value of t test.

Table 2. Brain Regions Showing Significant Activation During Imagery Task

	k[a]	BA	*t* score	Talairach Coordinates[b] x	y	z
Low Degrees of Alexithymia Group						
Past happy > REST						
Left posterior cingulate gyrus	325[c]	30	6.93	−4	−54	8
Past sad > REST						
Left superior frontal gyrus	229[c]	8	9.22	−4	22	48
Past neutral > REST						
Left anterior cingulate gyrus	128[d]	24	6.85	−3	4	47
Future happy > REST						
Left posterior cingulate gyrus	528[c]	30	9.85	−6	−54	9
Right posterior cingulate gyrus		30	6.25	6	−50	17
Right posterior cingulate gyrus		23	5.56	4	−58	14
Future happy > future neutral						
Right precuneus	97[d]	31	8.35	6	−62	25
High Degrees of Alexithymia Group						
Past happy > REST						
Left cerebellum anterior lobe	369[c]		10.54	−32	−48	−22
Left fusiform gyrus		37	7.81	−36	−60	−19
Left cerebellum posterior lobe			6.63	−31	−63	−25
Past neutral > REST						
Right cerebellum posterior lobe	398[c]		10.48	38	−73	−20
Right fusiform gyrus		18	6.40	24	−85	−19
Right cerebellum posterior lobe			5.75	19	−75	−22
Left fusiform gyrus[c]	179[c]	18	5.75	−20	−85	−20
Left cerebellum posterior lobe			4.76	−36	−73	−23
Future Happy > REST						
Left cerebellum anterior lobe[c]	566[c]		9.25	−36	−40	−30
Left cerebellum posterior lobe			6.78	−29	−75	−24
Left fusiform gyrus		19	5.81	−41	−75	−11

BA, Brodmann's Area; REST, during a rest condition.
[a]Number of voxels in cluster.
[b]Coordinates of the local points of maximal activation included in the cluster.
[c]Differences were significant at $p < .001$ (uncorrected) for voxel level and $p < .05$ (corrected) for cluster extent.
[d]Differences were significant at $p < .001$ (uncorrected) for voxel level and $p < .05$ (uncorrected) for cluster extent.

group showed significantly greater activity of the MPFC, which also extends to the ACC, during PS imagery, but the HDA group did not. This is partially in line with the ACC deficit model of alexithymia (Berthoz et al 2002; Lane et al 1997). There seems to be greater activation in the fusiform gyrus and cerebellum in the HDA group than in the LDA group, which might reflect visual attention (Allen et al 1997; Mangun et al 1998); however, such a comparison does not allow us to measure voxel-by-voxel differences in the magnitude of activation between the groups. A more formal test of the null hypothesis of no between-group difference in activation was provided by a two-sample *t* test at each voxel. A direct comparison between the groups showed significantly lower brain activation in the PCC of the HDA group than in that of the LDA group during FH imagery.

Table 3. Brain Regions Showing Significant Activation in Nonalexithymic Group Compared with Alexithymic Group During Imagery Task

Area	k[a]	BA	*t* score	Talairach Coordinates[b] x	y	z
Past Happy > REST						
Left posterior cingulate gyrus	220[c]	30	4.53	−4	−56	7
Left posterior cingulate gyrus		31	4.23	−1	−60	25
Left posterior cingulate gyrus		23	3.93	−8	−58	18
Future Happy > REST						
Left posterior cingulate gyrus	1150[d]	30	6.97	−4	22	48
Right posterior cingulate gyrus		31	5.61	8	−54	25
Future Happy > Future Neutral						
Right posterior cingulate gyrus	277[c]	31	5.58	6	−59	23

BA, Brodmann's Area; REST, during a rest condition.
[a]Number of voxels in cluster.
[b]Coordinates of the local points of maximal activation included in the cluster.
[c]Differences were significant at $p < .001$ (uncorrected) for voxel level and $p < .05$ (uncorrected) for cluster extent.
[d]Differences were significant at $p < .001$ (uncorrected) for voxel level and $p < .05$ (corrected) for cluster extent.